Developmental Biology
Genetics and Genomics

# The robust, high-throughput, and temporally regulated roxCre and loxCre reporting systems for genetic modifications *in vivo*

**Reviewed Preprint**
**v1** • June 13, 2024
Not revised

**Mengyang Shi, Jie Li, Xiuxiu Liu, Kuo Liu, Wenjuan Pu, Wendong Weng, Shaohua Zhang, Huan Zhao, Kathy O. Lui, Bin Zhou**

New Cornerstone Science Laboratory, State Key Laboratory of Cell Biology, CAS Center for Excellence in Molecular Cell Science, Shanghai Institute of Biochemistry and Cell Biology, Chinese Academy of Sciences, University of Chinese Academy of Sciences, Shanghai, China • Key Laboratory of Systems Health Science of Zhejiang Province, School of Life Science, Hangzhou Institute for Advanced Study, University of Chinese Academy of Sciences, Hangzhou, Chinace • Department of Chemical Pathology; and Li Ka Shing Institute of Health Sciences, The Chinese University of Hong Kong, Prince of Wales Hospital, Hong Kong, China • School of Life Science and Technology, ShanghaiTech University, Shanghai, China



## Abstract

Cre-loxP technology, a cornerstone in fate mapping and in vivo gene function studies, faces challenges in achieving precise and efficient conditional mutagenesis through inducible systems. In this study, we introduce two innovative genetic tools designed to overcome these limitations. The first, loxCre, facilitates conditional gene targeting by allowing any CreER line to induce Cre expression with significantly enhanced efficiency. The second, roxCre, enables DreER-mediated Cre release, paving the way for intersectional genetic manipulation that permits both increased precision and efficiency. Both tools incorporate a fluorescent reporter for genetic lineage tracing, revealing efficient gene knockout in cells marked by the reporter simultaneously. These strategies hold great potential for precise and efficient exploration of lineage-specific gene functions, marking a significant advancement in genetic research methodologies.

**eLife assessment:**

This study describes a new set of genetic tools for optimized Cre-mediated gene deletion in mice. The advances are substantial and will facilitate biomedical research. Although the tools have been validated using **solid** methodologies, the quantitative assessment of their recombination efficiency is not yet sufficiently described. Evaluating their ability to mediate the deletion of multiple alleles in a mosaic setting would also be a highly **valuable** addition.

https://doi.org/10.7554/eLife.97717.1.sa3

## Introduction

Genetic modification such as gene knockout in a precise spatiotemporal manner forms the basis for understanding cellular and molecular mechanisms in multiple biological processes[1, 2]. The powerful Cre-loxP recombination system is the most widely used approach employed to knockout or over-express specific genes *in vivo*[3]. Cre recombinase, derived from bacteriophage P1 gene, targets short palindrome DNA sequence loxP (34bp) and recombines two loxP-flanked sequences for deletion[4, 5]. Application of the Cre-loxP system in mouse genetics has revolutionized gene functional analysis and significantly advanced our understanding of many developmental and pathophysiological processes at the molecular level[6, 7]. To date, most of the mouse genes have been successfully targeted by two loxP sites (floxed allele), which could be recombined by cell-type specific Cre lines. For many *in vivo* genetic studies, a tissue-specific gene knockout approach has been widely used as a gold standard to dissect gene function in a particular cell type during a biological process.

While constitutively active Cre is robust and efficient in recombination for gene deletion, Cre lacks temporal control when the promoter driving Cre is active from the embryonic to the adult stage. Therefore, a temporally active Cre is needed to avoid early mortality as a result of the ablation of an indispensable gene at a key developmental stage. To overcome the temporal limitation of Cre, CreER, the fusion of Cre with a mutated estrogen receptor, is generated to enable its activation only after tamoxifen (Tam) treatment, and interaction of ER with Tam induces nuclear translocation of CreER from the cytoplasm[8]. As a result, the activity of inducible CreER could be controlled by Tam treatment, thus restricting CreER activity at a specific time window and permitting gene functional analysis at a higher spatiotemporal resolution than Cre[9]. As the loxP-flanked sequences and their locations in genome or chromatin influence its accessibility for recombination, the recombination efficiency of CreER varies significantly among different floxed alleles, ranging from easy-to inert-to-recombine alleles[10]. For example, CreER has high efficiency in targeting the easy-to-recombine alleles such as generic reporter *R26-tdT*[11], but exhibits low efficiency on some other reporters such as *R26-Confetti*[12], or may not excise some floxed gene alleles that are inert or resistant for targeting, leading to failure of gene deletion in some $tdT^+$ cells and causing false-positive tracing fate (**Figure 1A**). In other words, tdT expression may not always necessarily denote gene deletion in the labeled cells. The notion that the pattern of Cre-expression based on a reporter (e.g. *R26-tdT*) represents the pattern of Cre-mediated recombination is less rigorous[13]. It is therefore not correct to assume the successful deletion of the gene of interest based on the deletion of another gene (or reporter) by the same CreER mouse line.

One way to increase the recombination efficiency of CreER is to treat mice with many times of Tam, as the high dosage of Tam in theory could increase the chances of CreER-mediated recombination. However, the increased dosage of Tam treatment is toxic and could lead to many side effects on the phenotype, creating confounding effects on the study[14, 15]. To increase the inducible recombination efficiency of floxed alleles, Lao et al. reported a mosaic mutant analysis with spatial and temporal control of recombination (MASTR), in which initial FlpoER-mediated recombination induces GFPCre expression, that subsequently recombines floxed alleles effectively in $GFP^+$ cells[16]. Similarly, a Flp-induced mosaic analysis system with Cre or Tomato (MASCOT) has been reported to express Cre and reporter simultaneously in a cell[17]. While MASTR and MASCOT enable spatiotemporal labeling of mosaic mutant cells utilizing the current resources of floxed mouse lines, it may not be suitable for effective gene knockout at a tissue/population level due to low recombination efficiency initiated by Flp recombinase. In order to improve the inducible recombination efficiency, Tian et al. have also reported a self-cleaved inducible CreER (sCreER) that switches inducible CreER into a constitutively active Cre, effectively recombining floxed allele for gene manipulation[10]. However, self-cleaved inducible Cre mice have to be

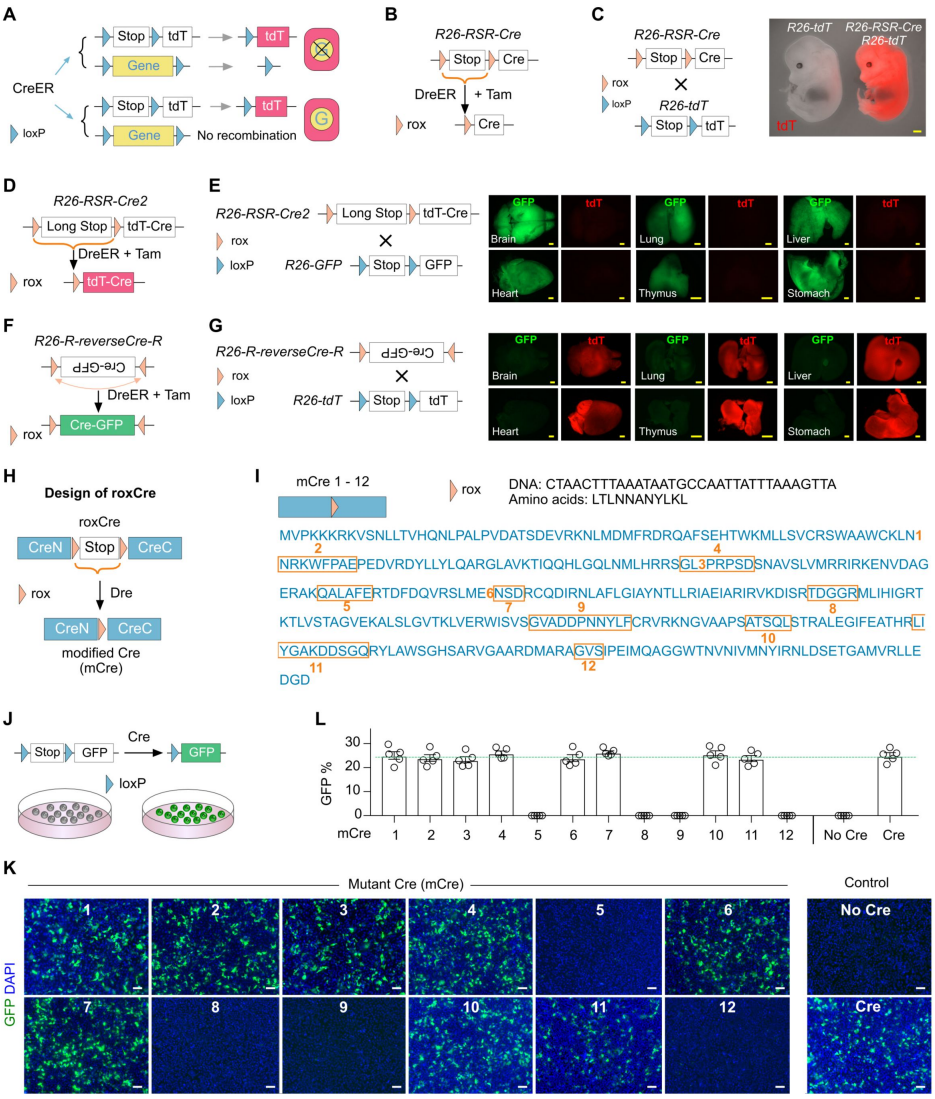


## Figure 1.

### Design of roxCre for DreER-induced mCre expression

(A) A schematic showing genetic labeling and/or gene knockout in CreER-expressing cells. (B, D, F) Strategies for DreER-induced Cre expression.

(C) Crossing with R26-tdT mice, R26-RSR-Cre exhibits leakiness in E13.5 embryos. Scale bars, yellow 1mm. Each image is representative of 5 individual biological samples.

(E) Examination of Cre leakiness by whole-mount fluorescence images of organs collected from R26-RSR-Cre2;R26-26-GFP adult mice. Scale bars, yellow 1mm. Each image is representative of 5 individual biological samples.

(G) Examination of Cre leakiness by whole-mount fluorescence images of organs collected from R26-R-reverseCre-R;R26-tdT adult mice. Scale bars, yellow 1mm. Each image is representative of 5 individual biological samples.

(H) A schematic showing the design for roxCre and mCre.

(I) A schematic showing mCre1 to mCre12 by insertion of rox into Cre cDNA at 12 different loci. Two dual-recombinase designs for inducible Cre expression once tried before.

(J) Examination of mCre for recombination efficiency by the *loxP-Stop-loxP-GFP* reporter.

(K) Immunofluorescence images of cells stained with GFP on cells. Scale bars, white, 100 μm. Each image is representative of 5 individual biological samples.

(L) Quantification of the percentage of cells expressing GFP in each group. Data are the means ± SEM; n = 5.

newly generated each time for targeting different promoters, which is time-consuming and the system is not compatible with current resources largely based on CreER mouse lines. A recent study has reported an iSuRe-Cre strategy to induce and report Cre-dependent genetic modifications utilizing conventional CreER tools[18]. The reporter expression reflects gene knockout in cells by *iSuRe-Cre*. However, two limitations hinder its widespread applications. First, without any induction, the *iSuRe-Cre* transgene is leaky in some tissues such as heart and skeletal muscle. Second, the initial recombination for releasing the *iSuRe-Cre* allele induced by CreER is far from efficient in some tissues compared with easy-to-recombine alleles such as *R26-tdT*[18], limiting its usage for efficient gene knockout at a tissue level. Thus, a new method is needed to ensure gene knockout in cells as effectively and efficiently as recombination on easy-to-recombine alleles, thus allowing efficient gene deletion at a population level.

Conventional Cre-loxP system uses tissue-specific promoter to drive Cre, thus the precision of genetic targeting solely depends on promoter activity. Now it is known that many promoters are not as specific as previously reported[19–21]. The ectopic or unwanted Cre expression in other cell types may result in unspecific cell labeling or gene deletion, leading to many confounding issues or controversies in multiple fields of research[22–24]. In addition, some cell types cannot be clearly distinguished by one marker from another, and thus could not be specifically and genetically targeted by only one gene promoter-driven recombinase[25]. To circumvent this limit, dual recombinases-mediated genetic targeting utilizes two promoters to independently drive Cre and Dre[26]. Dre is another bacteriophage recombinase that targets rox sites and is orthogonal to the Cre-loxP system[27]. While cells of interest could be labeled by specific reporters that are responsive to dual recombinases, gene deletion requires a final readout on singular Cre recombinase for targeting floxed gene alleles.

In this study, we developed two genetic strategies: roxCre and loxCre, in which the *rox-Stop-rox* (RSR) and *loxP-Stop-loxP* cassettes are respectively inserted into the *Cre* coding region, such that Cre transcription and translation are not properly carried out before the removal of the *Stop* cassette. We did not detect any spontaneous leakiness by roxCre or loxCre. We found that CreER-induced loxCre effectively deletes genes in reporter-labeled cells, ensuring efficient gene knockout for the evaluation of lineage-specific gene function. In addition, DreER-induced roxCre efficiently deletes genes in cells for both specific and efficient intersectional genetic studies. We expect that these tools would overcome the issues of inefficient and non-specific genetic modifications, enhancing our ability to more precisely manipulate genes in a particular cell lineage for a better understanding of gene functions in multiple biomedical fields.

# Results

## Design of roxCre for DreER-induced mCre expression

A sequential genetic approach has been recently reported to delete genes[28], which uses Dre-induced CreER expression by removing the *loxP-Stop-loxP* sequence ahead. As aforementioned, the recombination carried out by the released CreER for excising floxed gene alleles may not be as efficient as reporters (e.g. *R26-tdT*). A possible strategy to control Cre activity is to engineer a rox-flanked *Stop* sequence ahead of its DNA (*R26-RSR-Cre*) that will be removed after Dre-rox recombination (**Figure 1B**). However, such a strategy is not ideal, as the upstream transcriptional *Stop* sequence might not completely prevent *Cre* transcription, leading to the leakiness issue associated with the *iSuRe-Cre* strategy[18], for instance (**Figure 1C**). We then inserted a longer *Stop* sequence or reversed the direction of the *Cre* DNA by generating *R26-RSR-Cre2* and *R26-R-reverseCre-R* lines, respectively, that still displayed heavy leakiness as Cre was independently activated for recombination without being crossed with a Dre mouse line (**Figure**

**1D-G**). To enable efficient dual recombinases-mediated gene knockout, we need to design a strategy for DreER-induced expression of a constitutively active Cre, and the system should not exhibit leakiness.

We first generated roxCre, in which an RSR cassette was inserted into the coding region of *Cre*, splitting *Cre* into N- and C-terminal segments (**Figure 1H**). After removal of RSR by Dre-rox recombination, Cre is recombined containing one remaining rox site within its coding sequence, hereafter termed as modified Cre (mCre, **Figure 1H**). To ensure that mCre has the same recombination efficiency as a conventional Cre, we inserted a rox sequence at 12 different sites of *Cre* individually, most of which were located between helix domains (**Figure 1I**). As insertions of additional amino acids of rox would change the original sequence of Cre, potentially leading to reduced activity, we screened for their recombination efficiency by transfecting cells with 12 versions of mCre (mCre1 to mCre12) and the responding GFP reporter (**Figure 1J**). We found that mCre1, 2, 3, 4, 6, 7, 10, and 11 displayed a comparable efficiency as the conventional Cre; whereas mCre5, 8, 9, and 12 exhibited impaired recombination efficiency (**Figure 1K**, L). These data demonstrate that at least some of the mCre generated in our study were as efficient as the conventional Cre *in vitro*.

Next, we sought to screen for the most robust version of mCre *in vivo.* We generated four roxCre knock-in mice based on mCre1, 4, 7, and 10 as determined from the above *in vitro* screening (Figure S1-S2). In these roxCre lines, RSR inserted into *Cre* was removed by Dre-rox recombination resulting in the generation of mCre (**Figure 1J**). We then used hepatocyte- and endothelial cell-specific promoters albumin (Alb) and VE-cadherin (Cdh5) to drive roxCre, and generate *Alb-roxCre1-tdT*, *Cdh5-roxCre4-tdT*, *Alb-roxCre7-GFP*, and *Cdh5-roxCre10-GFP* knock-in mice, respectively (Figure S1-S2). No fluorescence signal was detected in *Alb-roxCre1-tdT*, *Cdh5-roxCre4-tdT*, *Alb-roxCre7-GFP*, and *Cdh5-roxCre10-GFP* knock-in mice (Figure S1-S2), demonstrating no reporter leakiness without Dre-rox recombination. These mice were crossed with *R26-GFP*[29] or *R26-tdT*[11] reporters. Nor did we detect leakiness as a result of any Cre activity when they were crossed with *R26-tdT* or *R26-GFP* reporter (Figure S1-S2). These data demonstrate that roxCre was functionally efficient yet non-leaky.

## DreER-induced mCre robustly recombines inert alleles

The mCre system was originally designed for inducible gene knockout to study biological functions. To more rigorously evaluate the recombination effectiveness among different versions of mCre, we used an inducible DreER to temporally and specifically release mCre in hepatocytes or endothelial cells. Although mCre efficiently labeled virtually all targeted cells (Figure S3A-E), a strong Cre is not needed to drive easy-to-recombine alleles such as *R26-tdT* reporter in this case. To identify a strong mCre, we attempted to target one of the most inert alleles for recombination, *R26-Confetti*[12], which is often used as reporters for clonal analysis due to its sparse labeling with rare recombination events[10, 12]. In the Cre-loxp recombination principle, Cre can remove the sequence between two loxp sites that have the same transcription direction and turn over the sequence in the middle of two loxp sites that have the opposite transcription direction. As the recombination efficiency of CreER is limited, *R26-Confetti* only can be recombined into YFP, or nGFP (nuclear GFP), or mCFP (membrane CFP), or RFP (Figure S3F).

We first crossed *R26-DreER;R26-Confetti* mice with *Alb-roxCre1-tdT* (group 1) and *Alb-roxCre7-GFP* (group 2) mice, and Tam-induced Dre-rox recombination yielded *Alb-mCre1-tdT* and *Alb-mCre7-GFP* mice, respectively (**Figure 2A**). In this system, the constitutively active mCre would completely remove the sequence between two loxp sites that have the same transcription direction, and recombine *R26-Confetti* into two sets of reporter pairs: YFP-nGFP pair and mCFP-RFP pair, which could be detected in a single hepatocyte due to the poly-nuclear or polyploidy feature of hepatocytes (**Figure 2A**). In each pair, reporters can equally express, as mCre is strong enough to turn over the sequence in the middle of two loxp sites that have the opposite transcription direction (Figure S3G). Therefore, we used YFP/mCFP to detect mCre recombination

efficiency and tdT/RFP or GFP to trace its endogenous reporter activity that was driven by Alb promoter in *Alb-mCre1-tdT* and *Alb-mCre7-GFP* mice, respectively (**Figure 2A**). Besides, *Alb-CreER*[26];*R26-Confetti* was used as a control under the same Tam treatment (group 3, **Figure 2A**).

In fact, DreER-rox recombination in hepatocytes is not 100%. Therefore, we quantified YFP and mCFP expression in hepatocytes with DreER-rox recombination to evaluate the strength of mCre activity. We found sparse $YFP^+$ or $mCFP^+$ hepatocytes (0.39 ± 0.04%) in *Alb-CreER;R26-Confetti* mice. On the other hand, 99.94 ± 0.02% of $tdT^+$ hepatocytes (DreER recombined) were $YFP^+$ or $mCFP^+$ in *R26-DreER;Alb-roxCre1-tdT;R26-Confetti* mice; and 76.83 ± 3.20% of $GFP^+$ hepatocytes (DreER recombined) were $YFP^+$ or $mCFP^+$ in *R26-DreER;Alb-roxCre7-GFP;R26-Confetti* mice (**Figure 2B**, C). Similarly, we found that 39.81 ± 2.61% of $tdT^+$ endothelial cells and 74.15 ± 3.64% of $GFP^+$ endothelial cells in small intestine were $YFP^+$ or $mCFP^+$ in *R26-DreER;Cdh5-roxCre4-tdT;R26-Confetti* and *R26-DreER;Cdh5-roxCre10-GFP;R26-Confetti* mice, respectively, compared with sparse labeling in *Cdh5-CreER;R26-Confetti* mice (**Figure 2D-F**). Similar results were also observed in other tissues and organs (Figure S4). These data demonstrate that inducible DreER controlled roxCre activation, and mCre1 was the most efficient recombinase assisting the recombination of inert alleles *in vivo*.

## Dre-induced mCre efficiently deletes floxed genes

Next, we examined the efficiency of gene knockout by Dre-induced mCre. We generated the *Alb-roxCre1-tdT;Ctnnb1*$^{flox/flox}$mouse line to examine if Dre-induced mCre could efficiently delete *Ctnnb1* gene that encodes β-catenin ($Ctnnb1^{flox}$)[30]. To enhance the precision and specificity of targeted cells, we employed intersectional genetic targeting using dual recombinases, and generated the *Cyp2e1-DreER* mouse line that labeled peri-central hepatocytes and also renal epithelial cells (Figure S5). Crossing *Cyp2e1-DreER* with hepatocyte-specific *Alb-roxCre1-tdT* mice achieved genetic targeting of peri-central hepatocytes exclusively, circumventing issues associated with ectopic targeting of renal cells by *Cyp2e1-DreER* line (Figure S5) or unwanted targeting of peri-portal hepatocytes by *Alb-CreER* line[26].

We generated *Cyp2e1-DreER;Alb-roxCre1-tdT;Ctnnb1*$^{flox/flox}$triple knock-in mice (mutant), in which Tam-induced DreER-rox recombination yielded mCre that subsequently targeted floxed Ctnnb1 allele (**Figure 3A**). We treated mutant mice and their littermate control *Cyp2e1-DreER;Alb-roxCre1-tdT;Ctnnb1*$^{flox/+}$ mice with Tam at 8 weeks of age, and purified $tdT^+$ hepatocytes for analysis at 3 days after Tam treatment (**Figure 3B**). qRT-PCR analysis showed significantly reduced *Ctnnb1* and *Glul* in $tdT^+$ hepatocytes of the mutant group, compared to that of the control group (**Figure 3C**, D). We then collected liver samples at 3 days (D) and 4 weeks (W) post-Tam for further analysis (**Figure 3E**). Immunostaining for tdT, β-catenin, GS, and E-CAD on liver sections revealed similar levels of β-catenin and GS expression in the 3D mutant liver than the control liver (**Figure 3F**). However, expression of β-catenin and GS almost disappeared in the 4W mutant sample compared with the control (**Figure 3G**), suggesting efficient deletion of *Ctnnb1* and down-regulation of Wnt signaling downstream gene target GS. Western blotting against β-catenin and qRT-PCR against *Ctnnb1* of purified $tdT^+$ hepatocytes at 4W post-Tam revealed a near complete loss of Ctnnb1 at both the protein and mRNA levels (**Figure 3H-K**). Additionally, Wnt downstream target genes including *Glul*, *Axin2*, *Cyp1a2*, *Cyp2e1*, *Oat*, *Tcf7*, *Lect2*, *Tbx3*, *Slc1a2*, and *Rhbg* were significantly reduced in the mutant than the control group (**Figure 3L**). Taken together, these data demonstrate that DreER-induced mCre enabled efficient intersectional genetic manipulation in the cells of interest.

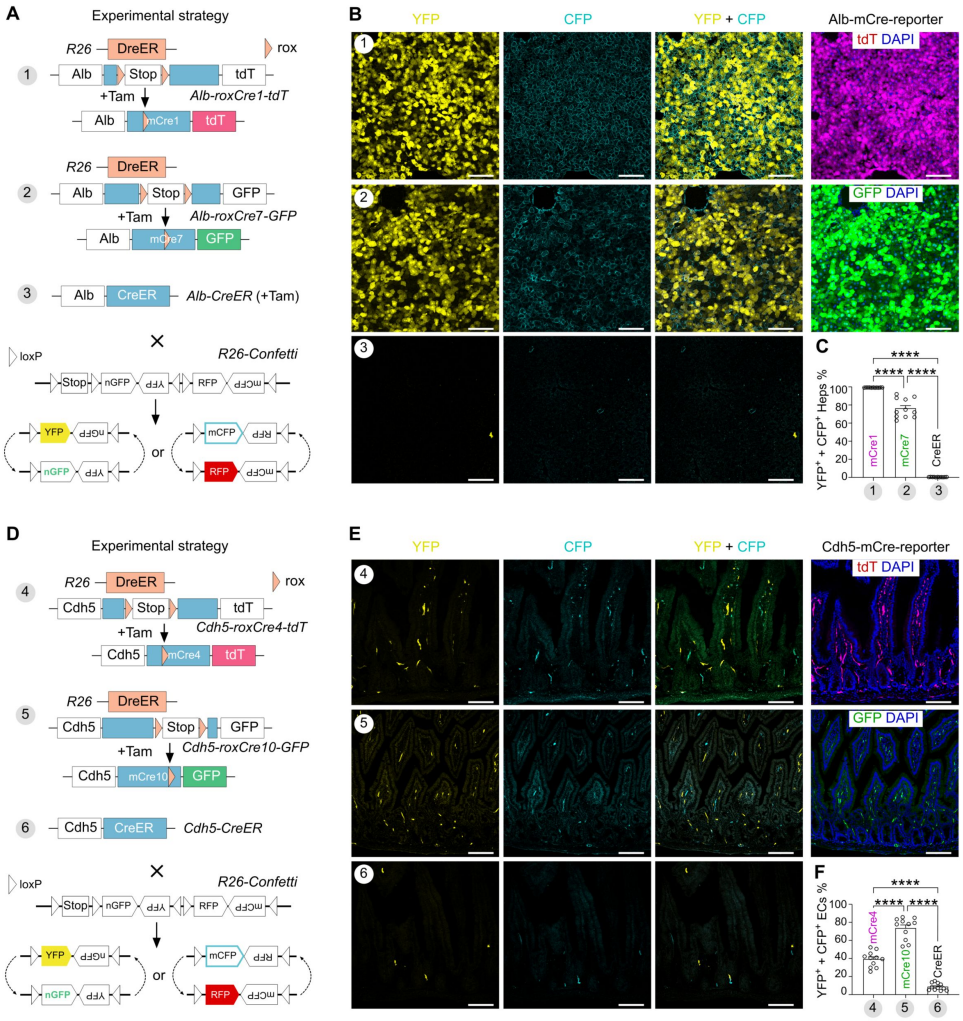


## Figure 2.

### DreER-induced mCre robustly recombines inert alleles

(A) A schematic showing the experimental design to test the recombination efficiency of mCre1 and mCre7 on the *R26-Confetti* allele. Tam-induced DreER-rox recombination leads to mCre1/tdT or mCre7/GFP expression in hepatocytes in strategy 1 or 2, respectively. Strategy 3 uses conventional *Alb-CreER* as control. YFP and mCFP signals are used for the examination of recombination on the *R26-Confetti* allele.

(B) Fluorescence images of YFP and mCFP on liver sections collected from mice in strategy 1-3. Strategy 1 and 3 exhibit tdT or GFP in hepatocytes after DreER-rox recombination, respectively. Scale bars, 100 μm. Each image is representative of 5 individual biological samples.

(C) Quantification of the percentage of hepatocytes (Heps) expressing either YFP and/or mCFP in strategy 4-6. Data are the means ± SEM; n = 11 mice for each strategy; ****$P < 0.0001$ by one-way ANOVA.

(D) A schematic showing the experimental strategy to test the recombination efficiency of mCre4 and mCre10 on *R26-Confetti* allele. Tam-induced recombination leads to mCre4/tdT or mCre10/GFP expression in endothelial cells (ECs) in strategy 4 or 5, respectively. Strategy 6 uses conventional *Cdh5-CreER* as control. YFP and mCFP signals are used for the examination of recombination on *R26-Confetti* allele.

(E) Fluorescence images of YFP and mCFP on intestinal sections collected from mice in strategy 4-6. Strategy 4 and 5 exhibit tdT or GFP in ECs after DreER-rox recombination, respectively. Scale bars, 100 μm. Each image is representative of 5 individual biological samples.

(F) Quantification of the percentage of ECs expressing either YFP and/or mCFP in strategy 4-6. Data are the means ± SEM; n = 11 mice for each strategy; ****$P < 0.0001$ by one-way ANOVA.

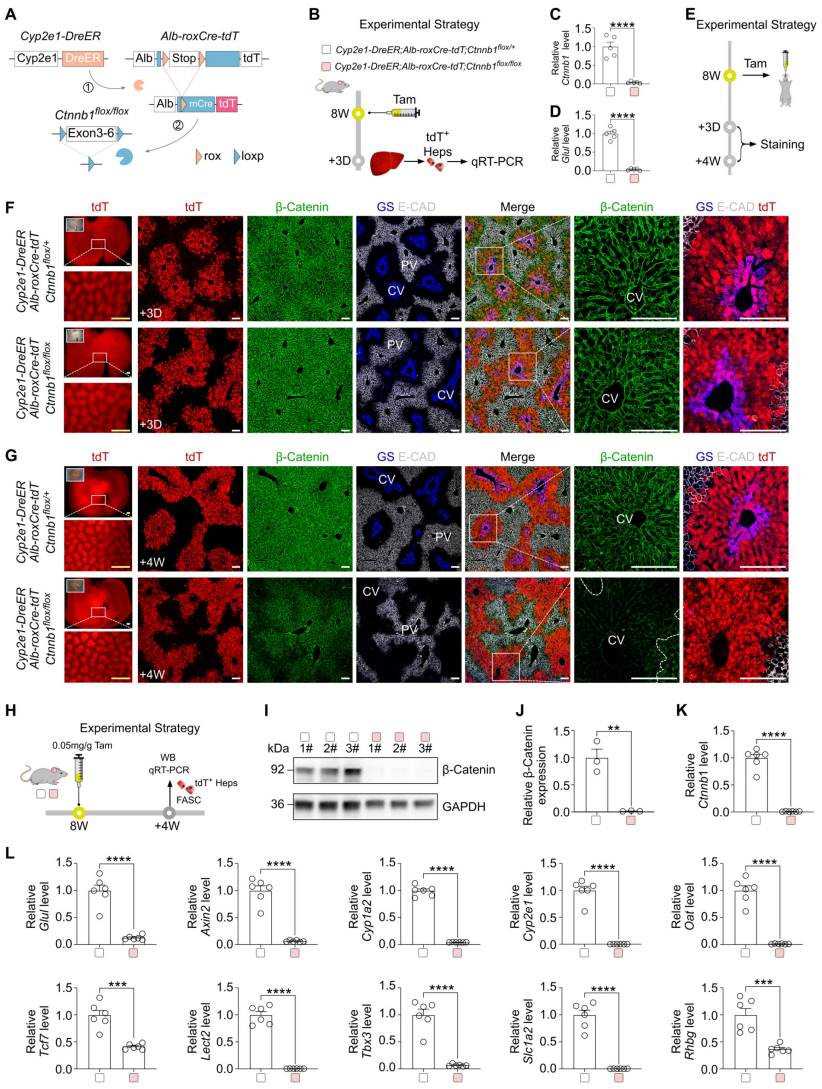

## Figure 3.

### Dre-induced mCre efficiently deletes genes

(A) A schematic showing the experimental design for Dre-induced mCre expression and the subsequent gene deletion.
(B) A schematic showing the experimental strategy.
(C and D) qRT-PCR analysis of the relative expression of *Ctnnb1* (C) and Glul (D) in the tdT$^+$ hepatocytes. Data are the means ± SEM; n = 5; ****$P$ < 0.0001 by student's $t$-test.
(E) A schematic showing the experimental strategy.
(F) Immunostaining for tdT, β-Catenin, GS, and E-CAD on liver sections collected on the day 3 post-Tam. PV, portal vein; CV, central vein. Scale bars, yellow 1mm; white 100 μm. Each image is representative of 5 individual biological samples.
(G) Immunostaining for tdT, β-Catenin, GS, and E-CAD on liver sections collected at week 4 post-Tam. Scale bars, yellow 1mm; white 100 μm. Each image is representative of 5 individual biological samples.
(H) A schematic showing the experimental strategy.
(I) Western blotting of β-Catenin and GAPDH in tdT$^+$ cells.
(J) Quantification of the relative expression of β-Catenin protein. Data are the means ± SEM; n = 3. **$P$ < 0.01 by student's $t$ test.
(K) qRT-PCR analysis of the relative expression of *Ctnnb1* in the tdT$^+$ cells. Data are the means ± SEM; n = 6. ****$P$ < 0.0001 by student's $t$ test.
(L) qRT-PCR analysis of the relative expression of *Glul*, *Axin2*, *Cyp1a2*, *Cyp2e1*, *Oat*, *Tcf7*, *Lect2*, *Tbx3*, *Slc1a2,* and *Rhbg* in the tdT$^+$ cells. Data are the means ± SEM; n = 6. ***$P$ < 0.001, ****$P$ < 0.0001 by student's $t$ test.

## *R26-loxCre-tdT* is efficiently recombined by CreER

Having successfully established roxCre1 for Dre-induced mCre expression, we iterated the system to enable mCre induction by CreER, a more widely available tool for biomedical research. We replaced the rox sites of roxCre1 with loxP sites by inserting a *loxP-Stop-loxP* cassette into *Cre* cDNA at the same locus as roxCre1(**Figure 4A**). We then generated a new *R26-loxCre-tdT* mouse line, in which mCre and tdT would be expressed simultaneously after *Stop* removal, allowing tdT as a surrogate marker for mCre detection in the same cell (**Figure 4C**). We then designed two experiments to verify the baseline leakiness of Cre expression (**Figure 4B**) and to examine if mCre/tdT could be expressed after *Stop* removal (**Figure 4C**), respectively, by *R26-loxCre-tdT;R26-tdT* (Strategy 1) and by injecting *AAV8-Cre* virus into *R26-loxCre-tdT* mice (Strategy 2). Immunostaining for tdT on tissue sections revealed no tdT expression in Strategy 1 demonstrating minimal to negligible leakiness at the baseline. The robust tdT expression in the liver in Strategy 2 showed mCre/tdT was allowed to express after *Stop* removal by AAV2/8-hTBG-Cre(**Figure 4D**).

We then confirm if the new design can improve the labeling efficiency compared to the conventional approach by crossing endothelial cell-specific *Cdh5-CreER* with the conventional reporter *R26-tdT* (Strategy 3) and the new reporter *R26-roxCre-tdT* mice (strategy 4) under the same protocol of Tam treatment (**Figure 4E**). Immunostaining for tdT and VE-Cad on tissue sections revealed no difference in the percentage of VE-Cad$^+$ endothelial cells expressing tdT between strategies 3 and 4 (**Figure 4F**-G), suggesting that recombination of the *R26-roxCre-tdT* allele by CreER was as efficient and easy as *R26-tdT* which is an easy-to-recombine reporter mouse line. Therefore, *R26-roxCre-tdT* can be served as an easy-to-recombine reporter, enabling efficient recombination to generate mCre/tdT in CreER-expressing cells, without leakiness.

## *R26-loxCre-tdT* adaptor ensures efficient recombination

We next examined whether mCre released from loxCre could also display high recombination efficiency for the inert-to-recombine allele *R26-Confetti*. We generated the triple knock-in *Cdh5-CreER;R26-loxCre-tdT;R26-Confetti* mouse line in which mCre was released for confetti recombination upon Tam treatment, and *Cdh5-CreER;R26-Confetti* was used as a control (**Figure 5A**). Both mouse strains were treated with Tam at 8 weeks of age and their tissue samples were collected for analysis at one week post-Tam (**Figure 5B**). As tdT expression is also detected in *R26-loxCre-tdT* after the first recombination by CreER, we only compared the YFP and mCFP fluorescence signals from *R26-Confetti* (**Figure 5A**). Wholemount-fluorescence imaging showed significantly more YFP and mCFP signals in the retina of the *Cdh5-CreER;R26-loxCre-tdT;R26-Confetti* mice, compared with that of *Cdh5-CreER;R26-Confetti* mice (**Figure 5C**). Immunostaining on frozen sections revealed significantly higher percentage of endothelial cells expressing YFP/mCFP in various vascularized organs of the *Cdh5-2a-CreER;R26-loxCre-tdT;R26-Confetti* mice, compared with that of the *Cdh5-2a-CreER;R26-Confetti* mice (**Figure 5D**). Of note, virtually all tdT$^+$ endothelial cells simultaneously expressed YFP/mCFP (**Figure 5D**). These data demonstrate that the *R26-loxCre-tdT* line could be used as an adaptor to enhance CreER-mediated recombination with a simultaneous expression of tdT as an accurate indicator.

## *R26-loxCre-tdT* ensures gene deletion in tdT$^+$ cells

To examine if *R26-roxCre-tdT* enables *Alb-CreER* to more efficiently delete genes, we crossed *Alb-CreER;R26-roxCre-tdT* with *Ctnnb1*$^{flox/flox}$to generate *Alb-CreER;R26-roxCre-tdT;Ctnnb1*$^{flox/flox}$ mice for evaluating the efficiency of releasing mCre and also mCre-mediated *Ctnnb1* deletion in tdT$^+$ hepatocytes (**Figure 6A**). We also crossed *Alb-CreER;R26-tdT2* with *Ctnnb1*$^{flox/flox}$ to generate *Alb-CreER;R26-tdT2;Ctnnb1*$^{flox/flox}$ mice to evaluate recombination efficiency of both *R26-tdT2* and *Ctnnb1*$^{flox/flox}$ alleles (**Figure 6A**). Additionally, *Alb-CreER;R26-roxCre-tdT;Ctnnb1*$^{flox/+}$ mice were used as a control for heterozygous gene deletion (**Figure 6B**). We treated *Alb-CreER;R26-*

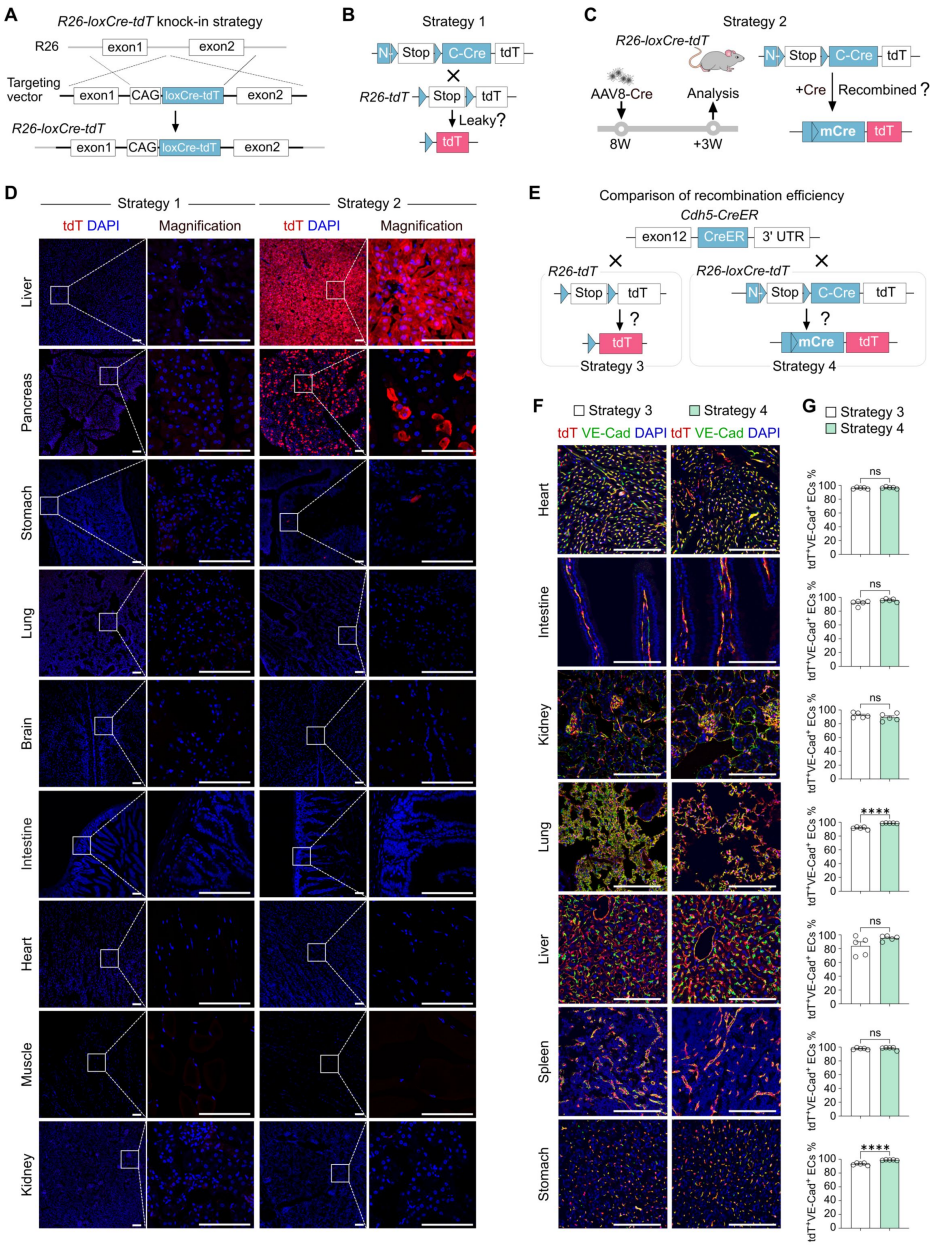


## Figure 4.

### *R26-loxCre-tdT* is efficiently recombined by CreER

(A) A schematic showing the knock-in strategy for the generation of the *R26-loxCre-tdT* allele. In this line, tdT is used to denote the mCre expression after the removal of *Stop*.
(B) A schematic showing the experimental strategy 1 to examine the leakiness of *R26-loxCre-tdT* mice.
(C) A schematic showing the experimental strategy 2 to test mCre/tdT expression by AAV8-TBG-Cre.
(D) Immunostaining for tdT on tissue sections shows tdT expression in the liver and pancreas when recombination was intiated by AAV8-TBG-Cre. Scale bars, white 100 μm. Each image is representative of 5 individual biological samples.
(E) A schematic showing the experimental strategies 3 and 4 for comparing the CreER-mediated first recombination efficiency between *Cdh5-CreER;R26-tdT* and *Cdh5-CreER;R26-loxCre-tdT* mice.
(F) Immunostaining for tdT and VE-Cad on liver sections collected on day 7 post-Tam. Scale bars, white 100 μm. Each image is representative of 5 individual biological samples.
(G) Quantification of the percentage of VE-Cad$^{+}$ ECs expressing tdT. Data are the means ± SEM; n= 6. ****$P$ < 0.0001 by student's *t*-test.

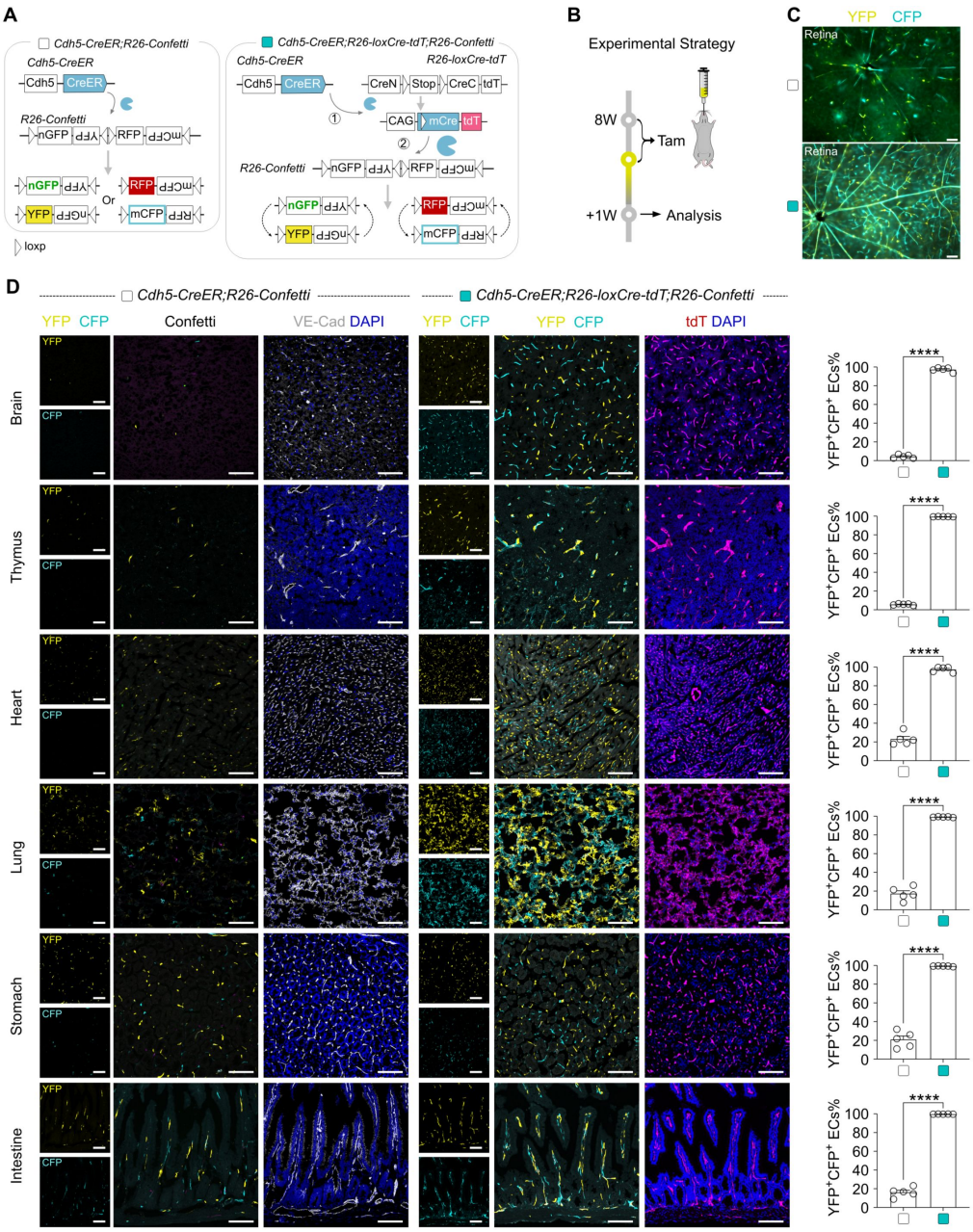


## Figure 5.

### *R26-loxCre-tdT* enables CreER to recombine *R26-Confetti* efficiently

(A) Schematics showing the experimental design. In *Cdh5-CreER;R26-loxCre-tdT;R26-Confetti* mice, Tam-induced CreER-loxp recombination switches *R26-loxCre-tdT* into *R26-mCre-tdT* allele with simultaneous tdT labeling and expression of mCre, which subsequently targets *R26-Confetti* (right panel). The conventional *Cdh5-CreER;R26-Confetti* mice are used as control.
(B) A schematic showing the experimental strategy.
(C) Whole-mount YFP and mCFP fluorescence images of retina collected from two mice groups. Scale bars, white 100 μm. Each image is representative of 5 individual biological samples.
(D) Immunofluorescence images of YFP, mCFP, and VE-Cad on tissue sections show significantly more $YFP^+$ and/or $mCFP^+$ ECs in the *Cdh5-CreER;R26-loxCre-tdT;Confetti* mice compared with that of *Cdh5-CreER;R26-Confetti* mice (left panel). The right panel shows the quantification of ECs expressing YFP and/or mCFP. Data are the means ± SEM; n = 5. ****$P < 0.0001$ by student's *t*-test. Scale bars, white 100 μm. Each image is representative of 5 individual biological samples.

*tdT2;Ctnnb1*$^{flox/flox}$ and *Alb-CreER;R26-roxCre-tdT;Ctnnb1*$^{flox/+}$ mice with five dosages of Tam, and treated *Alb-CreER;R26-roxCre-tdT;Ctnnb1*$^{flox/flox}$ mice only with one dosage of Tam, and collected tissues for analysis to determine *Ctnnb1* gene deletion at 4 weeks after Tam treatment (**Figure 6B**). Immunostaining data showed that β-catenin, GS, E-CAD, and Cyp2e1 were significantly reduced in *Alb-CreER;R26-roxCre-tdT;Ctnnb1*$^{flox/flox}$mice, but were readily detectable in both *Alb-CreER;R26-tdT2;Ctnnb1*$^{flox/flox}$and *Alb-CreER;R26-roxCre-tdT;Ctnnb1*$^{flox/+}$ mice (**Figure 6C**, D). Of note, a small number of hepatocytes continued to express Cyp2e1 in *Alb-CreER;R26-roxCre-tdT;Ctnnb1*$^{flox/flox}$ mice (**Figure 6D**). These Cyp2e1-expressing hepatocytes were unanimously tdT$^{-}$, and not a single tdT$^{+}$ hepatocyte expressed Cyp2e1 (**Figure 6D**), suggesting that these Cype2e1$^{+}$tdT$^{-}$ hepatocytes were likely not targeted by *Alb-CreER* for the recombination to release mCre. Western blotting of β-catenin and qRT-PCR of *Ctnnb1* of isolated hepatocytes revealed almost complete deletion of Ctnnb1 in the *Alb-CreER;R26-tdT2;Ctnnb1*$^{flox/flox}$mice compared with those in control groups (**Figure 6E-G**). Additionally, those Wnt downstream or regulated genes including *Glul*, *Axin2*, *Cyp1a2*, *Cyp2e1*, *Oat*, *Tcf7*, *Lect2*, *Tbx3*, *Slc1a2*, and *Rhbg* were significantly reduced in hepatocytes derived from the *Alb-CreER;R26-tdT2;Ctnnb1*$^{flox/flox}$mice, compared with those from the *Alb-CreER;R26-tdT2;Ctnnb1*$^{flox/flox}$and *Alb-CreER;R26-roxCre-tdT;Ctnnb1*$^{flox/+}$ mice, respectively (**Figure 6H**).

## Discussion

In this study, we respectively generated two genetic tools based on roxCre and loxCre to enhance the effectiveness of Cre-mediated gene deletion even under the control of a less efficient DreER or CreER driver. The *R26-loxCre-tdT* line permitted efficient recombination to release mCre, which greatly enhanced the effectiveness of subsequent gene deletion in tdT$^{+}$ cells. The inclusion of a fluorescent reporter with roxCre or loxCre allele allowed us to readily detect cells with gene deletion, thus facilitating further detailed characterization of these cells both *in situ* and *ex vivo*. Furthermore, the strategy of roxCre further enhances the precision for cell fate mapping with genetic deletion simultaneously in Dre$^{+}$Cre$^{+}$ cells through intersectional genetic targeting. For example, we have showcased the power of roxCre for genetic manipulation in peri-central hepatocytes, resulting in efficient gene knockout in tdT$^{+}$ hepatocytes specifically. Additionally, we have demonstrated the efficient deletion of *Wls* and *Ctnnb1* genes in tdT$^{+}$ endothelial cells and hepatocytes, respectively, by combining *R26-loxCre-tdT* adaptors with CreER lines. Altogether, we have demonstrated that the *R26-loxCre-tdT* mouse line could be widely applicable to any CreER-bearing mouse for enhancing its effectiveness in genetic modification with simultaneous cell lineage tracing in multiple biomedical research fields.

Coupling gene deletion with reporter activity can greatly facilitate the accuracy of studying gene function in targeted cells by *in situ* investigation with or without specific cell isolation for *ex vivo* experiments. Assuming successful gene deletion in the cell type of interest because of efficient cell labeling by a lineage-specific reporter mediated by the same Cre is incorrect, as recombination efficiency varies significantly among different mouse lines. In fact, many factors can potentially impact Cre-loxP recombination efficiency. Concerning the recombinase enzyme, the type of recombinase, the strength of the promoter that drives the recombinase, the expression level of the recombinase, and the translocation efficiency of an inducible recombinase such as CreER from the cytoplasm to the nucleus after Tam induction could all influence the recombination efficiency. For the targeted DNA sites, the genomic loci where targeted sites are placed, loxP-flanked sequence length, and even the inserted DNA sequence *per se* could also influence the recombination efficiency. We clearly observed the differences in recombination efficiency of different alleles (e.g. *R26-tdT*, *R26-tdT2*, and *R26-Confetti*), even located in the same genomic locus (e.g. Rosa26) mediated by the same CreER under the same Tam treatment protocol, as evidenced by high efficiency in *R26-tdT*, medium efficiency in *R26-tdT2*, and low efficiency in *R26-Confetti*. Importantly, *R26-loxCre-tdT* was found to be efficient for recombination mediated by CreER, which was comparable to that of the *R26-tdT* allele, thus enabling efficient labeling of cells of interest.

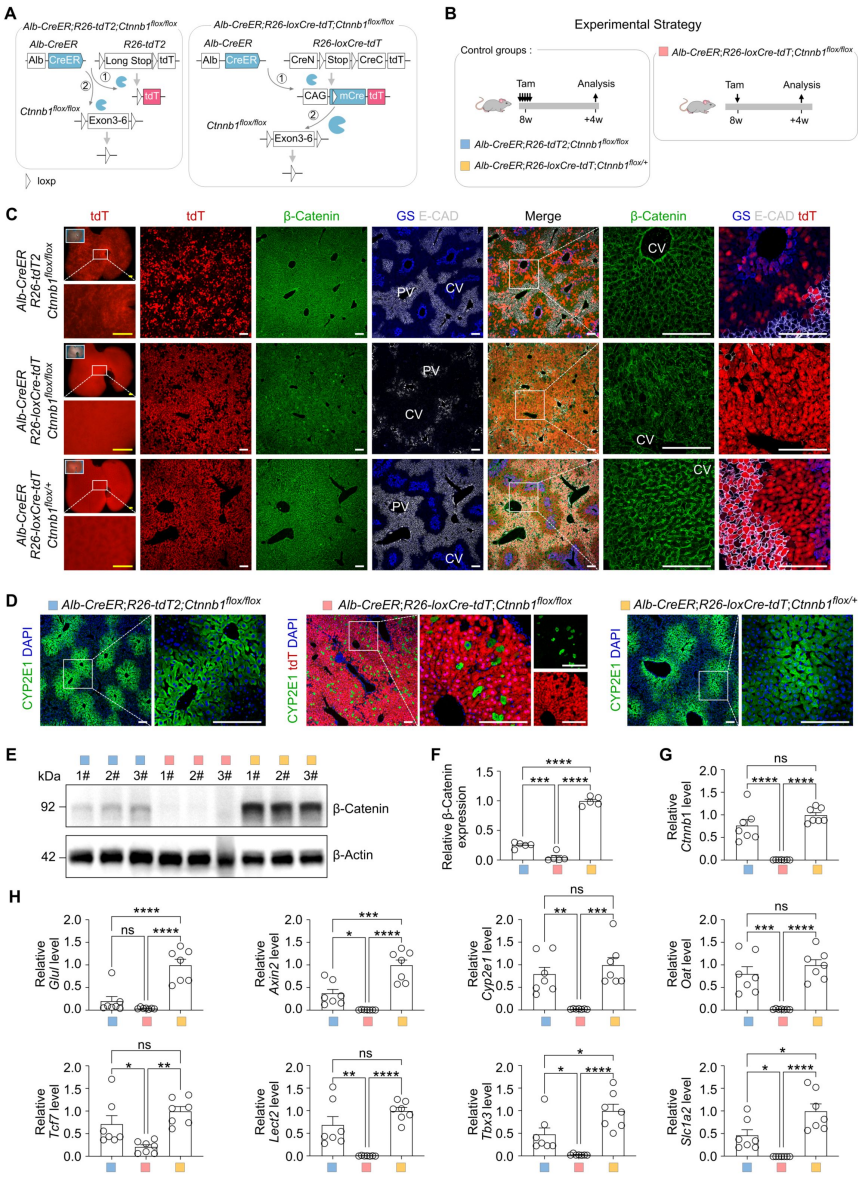


## Figure 6.

### *R26-loxCre-tdT* enables *Alb-CreER* to efficiently knockout genes in hepatocytes

(A) Schematics showing the experimental designs for Ctnnb1 gene knockout using either *Alb-CreER* or *Alb-CreER;R26-loxCre-tdT* mice.
(B) A schematic showing the experimental strategy. *Alb-CreER;R26-tdT2;Ctnnb1*$^{flox/flox}$ and *Alb-CreER;R26-loxCre-tdT;Ctnnb1*$^{flox/+}$ mice were injected with Tam for 5 times, while *Alb- CreER;R26-loxCre-tdT;Ctnnb1*$^{flox/flox}$ mice were injected with Tam for one time.
(C) Immunostaining for tdT, β-Catenin, GS, and E-CAD on liver sections. Scale bars, yellow 1mm; white 100 μm. Each image is representative of 5 individual biological samples.
(D) Immunostaining for tdT and CYP2E1 on liver sections. Scale bars, yellow 1mm; white 100 μm. Each image is representative of 5 individual biological samples.
(E) Western blotting of β-Catenin and β-Actin expression in hepatocytes, n = 3.
(F) Quantification of β-Catenin expression. Data are the means ± SEM; n = 5.
(G) qRT-PCR analysis of the relative expression of *Ctnnb1* in the hepatocytes.
(H) qRT-PCR analysis of the relative expression of *Glul*, *Axin2*, *Cyp2e1*, *Oat*, *Tcf7*, *Lect2*, *Tbx3*, and *Slc1a2* in hepatocytes. Data are the means ± SEM; n = 7; ns, non-significant; *$P$ < 0.05, **$P$ < 0.01, ***$P$ < 0.001, ****$P$ < 0.0001 by one-way ANOVA.

Furthermore, *R26-loxCre-tdT* also enabled CreER to efficiently ablate genes in any cells that had been genetically traced with tdT, synchronizing genetic modification and lineage tracing in the labeled cells.

Despite the high demand in the quest for efficient genetic modification in genetically labeled cells is significant, no efficient tool has been available to date. A previous study attempted to generate an adaptor for CreER to efficiently delete genes in reporter-labeled cells by a transgenic *iSuRe-Cre*[18]. However, the leakiness of *iSuRe-Cre* on the Rosa26 locus was too high in the male germline. Therefore, a transgenic mouse line was reconstructed subjected to *iSuRe-Cre* mediated recombination, which still displays consistently leaky recombination in some tissues such as cardiac and skeletal muscle[18]. The leakiness was likely due to the inability of the *Stop* cassette to completely block the transcription of *Cre* in *iSuRe-Cre*. Consistently, we also found leakiness as a result of *Cre* transcription even in the presence of *Stop* ahead in the *R26-Stop-Cre* mouse line (**Figure 1C**). These leaky events, despite being at different levels, demonstrate that transcription of recombinases such as Cre could not be easily inhibited. Instead of blocking its transcription by *Stop*, we inserted *Stop* in between the N- and C-terminus of *Cre*, thus preventing Cre expression completely at the translational level. We found that the removal of *Stop* rendered mCre, which efficiently recombined different types of alleles examined in our study. Additionally, we also observed inefficient recombination in hepatocyte-specific *Alb-CreER;iSuRe -Cre* mice, rendering this line less effective in conditional gene deletion in hepatocytes at a population level. In contrast, *R26-loxCre-tdT* was an easy-to-recombine allele for *Alb-CreER* mediated recombination, allowing tdT labeling and gene deletion simultaneously in the majority of hepatocytes. Therefore, our *R26-loxCre-tdT* line has circumvented the leakiness issue associated with *iSuRe-Cre*, exhibited as an easy-to-recombine allele for CreER targeting, and synchronized fate mapping with efficient genetic modification robustly, efficiently and temporally in the same cells.

The efficiency of CreER-loxP recombination depends not only on the location of the loxP-containing alleles but also on the strength of CreER driven by an active promoter. For instance, *R26-loxCre-tdT* was an easy-to-recombine allele compared with other tested R26 alleles, but the recombination efficiency to release mCre for subsequent recombination depends on the strength of the selected CreER lines for genetic targeting. It is known that different CreER mouse lines vary significantly for recombination, largely due to the differences in expression levels of CreER and Tam induction efficacy. Therefore, we should select a relatively stronger CreER line for efficient recombination on *R26-loxCre-tdT* to release mCre for gene deletion at a population level. In addition to bulk gene deletion, the *R26-loxCre-tdT* also offers an alternative way for mosaic analysis of gene function by sparse labeling. Previous studies have used Cre-loxP to over-express gene and fluorescence reporter simultaneously in a cell for functional genetic mosaic (ifgMosaic) analysis[31]. While ifgMosaic could over-express some dominantly negative genes for functional study, this system could not take advantage of rich resources from many conventionally available floxed mouse lines for loss-of-function study. Mosaic mutant analysis with spatial and temporal control of recombination (MASTR) utilized FlpoER for tissue-specific expression of GFPCre to delete floxed genes[16]. Compared with FlpoER lines, CreER is a more broadly used recombinase that most laboratories use in gene deletion experiments. A recent study using dual recombinase-mediated cassette exchange (MADR) also permits stable labeling of mutant cells expressing transgenic elements from defined chromosomal loci[32]. However, the use of viruses and electroporation, albeit convenient and rapid, are inefficient to specifically target any type of cells for *in vivo* studies. The powerful mosaic analysis with double markers (MADM) enables simultaneous lineage tracing of a pair of mutant and control sibling cells with distinct fluorescence reporters, allowing precise mosaic analysis of gene function in any cell[33, 34]. Nevertheless, the MADM cassette has to be combined with the mutant null allele, which is not readily available for synchronizing reporter expression and genetic modification in cells of interest. The ensured gene deletion with tdT reporter by *R26-roxCre-tdT* could be coupled with any present CreER and loxP alleles for potential mosaic analysis. This could be achieved by adjusting Tam at a lower dosage so that the recombination efficiency to release mCre could be low in cells of

interest for sparse tdT labeling. We believe that *R26-loxCre-tdT* could be useful for robust, efficient, and temporal gene deletion at a population level and mosaic analysis at a single-cell level with improvement in the future.

In this study, we deleted the Wnt signaling gene *Ctnnb1* in hepatocytes to present how roxCre and loxCre respectively enable efficient recombination. The impact of deleting *Ctnnb1* in a specific hepatocyte lineage on homeostasis, development, and injury recovery requires further investigation. Besides, roxCre and loxCre should be involved in more gene functional studies, in which knocking out genes continuously leads to embryonic death due to their crucial role in development.Both loxCre and roxCre incorporate a fluorescent reporter tdT for genetic lineage tracing, revealing efficient gene knockout in cells marked by the reporter simultaneously. In other words, one reporter tdT can only show cells with gene knockout. One direction to improve the current *R26-loxCre-tdT* for mosaic analysis in the future is to generate a second distinct surrogate reporter for wild-type cells as an internal control during mosaic analysis, similar to that in the MADM system.

# Materials and Methods

## Mice

Experiments using mice (Mus musculus) were carried out with the study protocols (SIBCB-S374-1702-001-C1) approved by the Institutional Animal Care and Use Committee of Center for Excellence in Molecular Cell Science (CEMCS), Shanghai Institute of Biochemistry and Cell Biology, Chinese Academy of Sciences. The *R26-DreER*[35], *Alb-CreER*[26], *R26-GFP*[29], *R26-tdT*[11], *R26-tdT2*[36], *R26-RSR-tdT*[37], *R26-Confetti*[12],and *Ctnnb1-flox*[30] mouse lines were used as previously described. New knock-in mouse lines *R26-RSR-Cre*, *R26-RSR-Cre2*, *R26-R-reverseCre-R*, *Cdh5-CreER*, *Alb-roxCre1-tdT*, *Alb-roxCre7-GFP*, *Cdh5-roxCre4-tdT*, *Cdh5-roxCre10-GFP*, *Cyp2e1-DreER*, and *R26-loxCre-tdT* were generated by homologous recombination using CRISPR/Cas9 technology. These new mouse lines were generated by the Shanghai Model Organisms Center, Inc. (SMOC). These mice were bred in a C57BL6/ICR mixed background. All mice were housed at the laboratory Animal center of the Center for Excellence in Molecular Cell Science in a Specific Pathogen Free facility with individually ventilated cages. The room has controlled temperature (20–25 °C), humidity (30–70%), and light (12 hours light-dark cycle). For the determination of the embryonic period of sampling, the day on which the vaginal plug was examined in female mice was recorded as E0.5. As the sex is not relevant to the topic of this study, male and female mice ranging in age from E13.5 to 12W (week) were allocated and mixed into the experimental groups in this study. No data in mouse experiments were excluded.

## Genomic PCR

Genomic DNA was prepared from the mouse toes or embryonic tails. Tissues were precipitated by centrifugation at maximum speed for 1 min at room temperature. After that, tissues were lysed by lysis buffer (100 mM Tris-HCl, 5 mM EDTA, 0.2% SDS, 200 mM NaCl, and 100 μg/mL Proteinase K) at 55 °C overnight. About 750μL pure ethanol was added to the lysis mixture and mixed thoroughly, followed by centrifugation at maximum speed for 5 min at room temperature to collect the DNA precipitation. Then the supernatant was discarded and the mixture was dried at 55 °C for 1 hour. About 100–200μL double-distilled $H_2O$ was added to dissolve the DNA. The genomic PCR primer pairs were designed for the mutant alleles spanning both endogenous genomic fragments and insert fragments. All the new genomic PCR primer sequences would be provided upon request.

## *In vitro* screening of mCre for efficient recombination

To test if the remaining rox sequence after Dre-rox recombination would impact Cre activity, the pCDNA3.1[38] (Invitrogen, V79020) was used to express 12 types of modified Cre (mCre). For testing the Cre activity, 500ng pCDNA3.1-mCre plasmids, or pCDNA3.1 (negative control), or pHR-CMV-nlsCRE (positive control, Invitrogen, 12265) were mixed with 500ng pCAG-loxp-stop-loxp-ZsGreen (Addgene, 51269) plasmid. *In-vitro* transfection experiment protocol is performed according to that described previously[39]. For cell culture medium, DMEM (ThermoFisher, 11965092) was supplemented with 10% fetal bovine serum (fetal bovine serum, 10099141c) for preparing fresh complete culture medium. Poly-D-Lysine (ThermoFisher, A3890401) precoated coverslips (biosharp, BS-14-RC) or 10 cm dish (ThermoFisher, 150466) overnight to dry, and sterile water was used to flush it for three times. A cryogenic vial of QBI293 was put in a 37°C water bath, then thawed liquid contents into a 50 mL conical tube (Corning,430829) prefilled with 5 mL prewarmed fresh complete culture medium. After centrifuging at 125 × g for 5 min, the supernatant was discarded and cells were resuspended in 10 mL complete medium. One-third of the cells were plated in a 10 cm coated dish and incubated in cultures at 37°C. On the second day, the culture medium was discarded, and the cell layer was briefly rinsed with prewarmed PBS (Gibco, C10010500BT). After that, PBS was removed and 1 mL 0.25% Trypsin solution (with EDTA, Gibco, 25200072) was added. The cells were incubated at 37°C for 3 min., and a 6mL complete growth medium was added to aspirate cells by gently pipetting. The medium-containing cells were transferred to a 50 mL conical tube and centrifuged at 125 × g for 5 min. The supernatant was discarded, and cells were resuspended in 5.2 mL complete culture medium. 24 well plates were placed into coated coverslips and added 1mL complete culture medium. 200μL cells were added to every experimental well and incubated cultures at 37°C for 9 hours to grow up to ~80%. The new prewarmed fresh complete culture medium replaced the old for 1mL per well. Lipofectamine™ 3000 Transfection Reagent (Thermo Fisher, L3000015) was used for plasmid transfection. Samples were incubated in cultures at 37°C for 24 hours. Samples were washed by PBS once and mounted on slides by VECTASHIELD®. Antifade Mounting Medium with DAPI (Vector, H-1200). Images were acquired using an Olympus microscope (Olympus, BX53).

## Tamoxifen injection and sample collection

For induction of CreER or DreER, tamoxifen (Sigma, T5648) was dissolved in corn oil and was administered to mice by oral gavage. *Cyp2e1-DreER;Alb-roxCre1-tdT;Ctnnb1*$^{flox/+}$and *Cyp2e1-DreER;Alb-roxCre1-tdT;Ctnnb1*$^{flox/flox}$ mice were treated with 0.05 mg Tam per gram mouse body weight for one dose. For comparing tdT$^{+}$ cells, *Cyp2e1-DreER;R26-RSR-tdT* and *Cyp2e1-DreER;Alb-roxCre1-tdT* mice were treated with 0.05 mg Tam per gram mouse body weight. *R26-DreER;Alb-roxCre1-tdT;R26-Confetti*, *R26-DreER;Cdh5-roxCre4-tdT;R26-Confetti*, *R26-DreER;Alb-roxCre7-GFP;R26-Confetti*, *R26-DreER;Cdh5-roxCre10-GFP;R26-Confetti*, *R26-DreER; R26-DreER;Alb-roxCre7-GFP;R26-GFP*, *Alb-CreER;R26-Confetti*, *Cdh5-CreER;R26-Confetti*, *Alb-CreER;R26-tdT2;R26-Confetti*, *Alb-CreER;iSuRe-Cre;R26-Confetti*, *Alb-CreER;R26-loxCre-tdT;R26-Confetti*, *Alb-CreER;R26-loxCre-tdT;Ctnnb1*$^{flox/flox}$, and *Cyp2e1-DreER;R26-RSR-tdT* mice were treated with 0.2 mg Tam per gram mouse body weight for one dose. *Cdh5-CreER;R26-tdT*, *Cdh5-CreER;R26-loxCre-tdT*, *Cdh5-CreER;R26-Confetti*, *Cdh5-CreER;R26-loxCre-tdT;R26-Confetti*, *Alb-CreER;R26-tdT2;Ctnnb1*$^{flox/flox}$, and *Alb-CreER;R26-loxCre-tdT;Ctnnb1*$^{flox/+}$ mice were treated with 0.2 mg Tam per gram mouse body weight one dose per day for 5 days. *R26-RSR-Cre2;R26-GFP* and *R26-R-reverseCre-R;R26-tdT* mice were sacrificed at 8 weeks old for analysis. Mice, both males and females, at the age of 8–12 weeks were used for experiments with similar-aged mice for both control and experimental groups.

## Whole-mount imaging and sectioning

The tissue samples were fixed with 4% paraformaldehyde (PFA) (Sigma, P6148-500g, wt/vol in PBS) for 1 or 2 hours (stomach, intestine, colon) at 4°C, followed by washing with PBS three times. The fixed tissues were placed in an agarose-filled petri dish for bright-field and fluorescence imaging by a Zeiss stereoscopic microscope (AxioZoom V16). For cryo-sections, tissues were sectioned to slides of 10-μm thickness after dehydration by 30% sucrose (Sinopharm, H-10021463, wt/vol in PBS) overnight and pre-embedding with OCT (Sakura) at 4 °C for 1 hour.

## Immunostaining

Immunostaining was performed as previously described[40]. 0.2% PBST was prepared with 0.2% (vol/vol) Triton X-100(Sigma, T9284) dissolved in PBS. Tissue sections were blocked with 2.5% normal donkey serum and 0.1% 4'6-diamidino-2-phenylindole (DAPI, Vector lab, D21490) dissolved in 0.2% PBST for 30 mins after washing with PBS three times. The tissue sections were incubated with primary antibody diluted in 0.2% PBST at 4°C overnight. On the next day, sections were incubated with secondary antibodies diluted in 0.2% PBST at room temperature for 30 min, followed by PBS washing for three times. The slides were washed with PBS for three times. The slides were mounted with a mounting medium (Vector Lab). For weak signals, the endogenous peroxidase activity was quenched before blocking. Horseradish peroxidase or biotin-conjugated secondary antibodies and a Tyramide signal amplification kit (PerkinElmer) were used after incubating the primary antibodies. For primary antibodies of murine origin, mouse immunoglobulins were blocked with an anti-mouse Fab antibody (Jackson, 715-007-003, 1:100). The included primary antibodies are listed as follows: tdT (Rockland, 600-401-379, 1:500; or Rockland, 200-101-379, 1:500), GFP (Invitrogen, A11122, 1:500), GFP (Rockland, 600-101-215M, 1:500), GFP (Nacalai, 04404-84; 1:500), GS (Abcam, ab49873, 1:1000), β-catenin (BD Pharmingen, 610153, 1:200), E-CAD (R&D, AF748, 1:500), Ep-CAM (Abcam, ab92382, 1:500), VE-Cad (R&D, AF1002, 1:100), and CYP2E1(Abcam, ab28146, 1:100). The corresponding secondary antibodies (JIR or Abcam) were diluted according to the instructions. Images were captured by using a Nikon confocal (Nikon A1 FLIM) or an Olympus confocal (FV3000), and captured images were analyzed by Image J2 (version 2.9.0/1.54f) and Photoline (version 23.02) software. We collected five random fields from each liver section for quantification. Mutant and control sections were processed at the same time to avoid potential batch differences during staining. Imaging of all immunostained slides was performed under the same exposure and contrast conditions using the same confocal microscope.

## Imaging of Confetti fluorescence reporters

All the fluorescence images of *R26-confetti* were taken by a Leica confocal (Leica SP8 will). All the sections were collected freshly and blocked with 0.2% PBST containing DAPI for 30 mins after washing with PBS three times. The parameters of excitement light and emission light for all channels are set as follows: DAPI (ex.405nm, em.415-450nm), CFP (ex.458nm, em.463-481nm), GFP (ex.488nm, em.495-511nm), YFP (ex.520nm, em.527-545nm), tdT (ex.546nm, em.555-590nm), markers for antibody staining (ex.647nm, em.657-700nm). Captured images were analyzed by Image J2 (version 2.9.0/1.54f) and Photoline (version 23.02) software.

## Hepatocyte dissociation

Mouse primary hepatocytes were isolated by the two-step collagenase perfusion method, which was modified from a previous protocol[41]. Briefly, mice were anesthetized and the liver was exposed through an incision in the lower abdomen. The inferior vena cava and portal vein were also exposed. A needle was inserted into the inferior vena cava and secured with a hemostatic clamp around the needle. The portal vein was cut immediately when the mouse liver was perfused with a perfusion medium buffer (containing 0.5 mM EGTA) for 5 minutes using a peristaltic pump. Then, the liver was perfused with medium containing collagenase type I (150 U/ml; Gibco, 17100-

017) for 2-5 min to adequately digest the liver. After the gallbladder was removed, the liver was dissected with cold DMEM to free the hepatic cells. Then the cell suspension was passed through a 70-μm cell strainer (BD Biosciences, 352350) and centrifuged at 50 x g for 3 min at 4 °C. The supernatant was removed, and cells were resuspended in Percoll (GE Healthcare, 17-0891-01)/DMEM/10 x PBS (Sangon, B548117, diluted in 1:1) (1:1:0.1) mixture and centrifuged at 300 x g for 5 min at 4 °C. After the supernatant was removed, cells were dissected with cold DMEM and centrifuged at 50 x g for 3 min at 4 °C. Purified hepatocytes were collected for FACS analysis, qRT-PCR or Western Blot analysis.

## Flow cytometric analysis and isolation of $tdT^+$ hepatocytes

Cells were stained with the following antibodies: anti-mouse CD45 APC (eBioscience, 17-0451-82, 1:400), anti-mouse CD140a APC (eBioscience, 17-1401-81, 1:100), anti-mouse CD31 APC (eBioscience, 17-0311-82, 1:40). All antibodies were diluted in 1~2mL DMEM (according to cells number) and cells were incubated with antibodies for 30 min in the dark at 4 °C. After staining, 10mL DMEM was added to stop staining, and the cell suspension was passed through a 70-μm cell strainer. Cells were centrifuged at 50 x g for 3 min at 4 °C and dissected with relevant suspended solution. For no DAPI control group, their suspended solution is 0.1% Dnase I (Worthington, LS002139, diluted by DMEM), otherwise, the suspended solution is 0.1% Dnase I mixed with 0.1% DAPI. Hepatocytes were sorted by FACS Aria SORP machine. Cell viability was assessed with DAPI staining. $APC^-tdT^+$ hepatocytes were collected for subsequent experiments.

## Total RNA extraction and qRT-PCR

Total RNA was extracted from the liver of indicated mice or hepatocytes isolated from indicated mice as previously described[42]. Cells or homogenized tissues were lysed with Trizol (Invitrogen, 15596018), and total RNA was extracted according to the manufacturer's instructions. For each sample, 1 μg of total RNA was reversely transcribed into cDNA using the Prime Script RT kit (Takara, RR047A). The SYBR Green qPCR master mix (Thermo Fisher Scientific, 4367659) was used and quantitative RT-PCR was performed on QuantStudio 6 Real-Time PCR System (Thermo Fisher Scientific). *Gapdh* was used as the internal control. Sequences of all primers would be provided upon request.

## Western blot

Liver tissues were collected at the indicated stages. All samples were lysed in RIPA lysis buffer (Beyotime, P0013B) containing protease inhibitors (Roche, 11836153001) for 30 min on ice, and then centrifuged at 15,000 x g for 15 min to collect the supernatant. All samples were separated with 30μL for testing the protein concentration by Pierce™ BCA Protein Assay kits (Thermo Scientific™,23227). The remaining samples were mixed with 5 x loading buffer (Beyotime, p0015L) and boiled at 100 °C for 5 min. 40μg samples were added to every well in precast gradient gels (Beyotime, P0469M) with 1x running buffer (Epizyme, PS105S, should be diluted into 1x). After running, samples were transferred onto Immobilon® PVDF membranes (Millipore, IPVH00010). After blocking in blocking buffer (Epizyme, PS108P), the membranes were incubated with primary antibodies (diluted by primary antibody dilution buffer (Epzyme, PS114)) overnight at 4 °C, then washed for three times and incubated with HRP-conjugated secondary antibodies (diluted by 1xTBST (Epzyme, PS103S, should be diluted into 1x)). Samples were incubated with chemiluminescent HRP substrate (Thermo Fisher Scientific, WBKLS0500), and related signals were detected by MiniChemi 610 Plus (Biogp). The following antibodies were used: β-catenin (BD Pharmingen, 610153, 1: 5000), GAPDH (Proteintech, 60004-1-IG, 1:2000), β-actin (Epzyme, LF202,1:1000), HRP-donkey-a-mouse (JIR, 715-035-150, 1:5000), and HRP-goat a rabbit IgG (JIR, 111-035-047, 1:5000).

### AAV injection

The AAVs used in this study were purchased from Taitool Biotechnologies company (Shanghai, China). Briefly, AAVs were produced with cis-plasmids containing the full TBG promoter, which is specifically active in hepatocytes, and Cre expression is under the control of TBG promoter, replication incompetent AAV2/8-TBG-Cre virus (AAV8-TBG-Cre, S0657-8-H5) was packaged and purified before application to mice. Mice were injected intraperitoneally at 1x $10^{11}$ genome copies of the virus per mouse. The above newly generated virus as well as targeting plasmids will be provided upon request.

### Statistical analysis

Statistical analyses were performed using GraphPad Prism (Version 9.5.1). All the continuous variables were expressed as means ± standard error of the mean (SEM). One-way ANOVA was used to detect statistical significance between three experimental groups. The statistical difference between the two experimental groups was determined using the unpaired student's *t*-test. The probability (*P*) values of less than 0.05 were considered statistically significant.

## Acknowledgements

This study was supported by the National Key Research & Development Program of China (2023YFA1800700, 2022YFA1104200, 2023YFA1801300, 2020YFA0803202), National Natural Science Foundation of China (82088101, 32370897, 32100648, 32370783, 32100592), CAS Project for Young Scientists in Basic Research (YSBR-012), Shanghai Pilot Program for Basic Research-CAS, Shanghai Branch (JCYJ-SHFY-2021-0), Research Funds of Hangzhou Institute for Advanced Study (2022ZZ01015, B04006C01600515), Shanghai Municipal Science and Technology Major Project, and the New Cornerstone Science Foundation through the New Cornerstone Investigator Program and the XPLORER PRIZE.

## Author contributions

M.S., J.L., and B.Z. designed the study, analyzed the data, and wrote the manuscript; X.L., K.L., W.P., W.W., S.Z., and H.Z. bred the mice and performed experiments; K.O.L. edited the manuscript and provided intellectual input; B.Z. conceived, supervised, and organized the study.

## Declaration of interests

The authors declare no competing interests.

## Data availability

All data included in this study are included in the manuscript. The raw data are available upon request.

# References


1. Gu H., Zou Y. R., Rajewsky K (1993) **Independent control of immunoglobulin switch recombination at individual switch regions evidenced through Cre-loxP-mediated gene targeting** *Cell* **73**:1155–1164

2. Gu H., Marth J. D., Orban P. C., Mossmann H., Rajewsky K (1994) **Deletion of a DNA polymerase beta gene segment in T cells using cell type-specific gene targeting** *Science* **265**:103–106 https://doi.org/10.1126/science.8016642

3. Nagy A (2000) **Cre recombinase: the universal reagent for genome tailoring** *Genesis* **26**:99–109

4. Sternberg N., Hamilton D., Austin S., Yarmolinsky M., Hoess R (1981) **Site-specific recombination and its role in the life cycle of bacteriophage P1** *Cold Spring Harb Symp Quant Biol* **45**:297–309

5. Sauer B., Henderson N (1988) **Site-specific DNA recombination in mammalian cells by the Cre recombinase of bacteriophage P1** *Proc Natl Acad Sci U S A* **85**:5166–5170

6. Orban P. C., Chui D., Marth J. D (1992) **Tissue- and site-specific DNA recombination in transgenic mice** *Proc Natl Acad Sci U S A* **89**:6861–6865

7. Lakso M., Sauer B., Mosinger B. J., Lee E. J., Manning R. W., Yu S. H., Mulder K. L., Westphal H (1992) **Targeted oncogene activation by site-specific recombination in transgenic mice** *Proc Natl Acad Sci U S A* **89**:6232–6236

8. Feil R., Wagner J., Metzger D., Chambon P (1997) **Regulation of Cre recombinase activity by mutated estrogen receptor ligand-binding domains** *Biochem Biophys Res Commun* **237**:752–757 https://doi.org/10.1006/bbrc.1997.7124

9. Tian X., Pu W. T., Zhou B (2015) **Cellular Origin and Developmental Program of Coronary Angiogenesis** *Circ Res* **116**:515–530 https://doi.org/10.1161/CIRCRESAHA.116.305097

10. Tian X. *et al.* (2020) **Generation of a self-cleaved inducible Cre recombinase for efficient temporal genetic manipulation** *EMBO J* **39** https://doi.org/10.15252/embj.2019102675

11. Madisen L. *et al.* (2010) **A robust and high-throughput Cre reporting and characterization system for the whole mouse brain** *Nat Neurosci* **13**:133–140 https://doi.org/10.1038/nn.2467

12. Snippert H. J. *et al.* (2010) **Intestinal crypt homeostasis results from neutral competition between symmetrically dividing Lgr5 stem cells** *Cell* **143**:134–144 https://doi.org/10.1016/j.cell.2010.09.016

13. Becher B., Waisman A., Lu L. F (2018) **Conditional Gene-Targeting in Mice: Problems and Solutions** *Immunity* **48**:835–836 https://doi.org/10.1016/j.immuni.2018.05.002

14. Brash J. T., Bolton R. L., Rashbrook V. S., Denti L., Kubota Y., Ruhrberg C (2020) **Tamoxifen-Activated CreERT Impairs Retinal Angiogenesis Independently of Gene Deletion** *Circ Res* **127**:849–850 https://doi.org/10.1161/CIRCRESAHA.120.317025

15. Rashbrook V. S., Brash J. T., Ruhrberg C (2022) **Cre toxicity in mouse models of cardiovascular physiology and disease** *Nat Cardiovasc Res* **1**:806–816 https://doi.org/10.1038/s44161-022-00125-6

16. Lao Z., Raju G. P., Bai C. B., Joyner A. L (2012) **MASTR: a technique for mosaic mutant analysis with spatial and temporal control of recombination using conditional floxed alleles in mice** *Cell Rep* **2**:386–396 https://doi.org/10.1016/j.celrep.2012.07.004

17. Wang Q. *et al.* (2020) **A mosaic analysis system with Cre or Tomato expression in the mouse** *Proc Natl Acad Sci U S A* **117**:28212–28220 https://doi.org/10.1073/pnas.2014308117

18. Fernández-Chacón M., Casquero-García V., Luo W., Francesca Lunella F., Ferreira Rocha S., Del Olmo-Cabrera S., Benedito R (2019) **iSuRe-Cre is a genetic tool to reliably induce and report Cre-dependent genetic modifications** *Nat Commun* **10** https://doi.org/10.1038/s41467-019-10239-4

19. Liu Q. *et al.* (2016) **Genetic lineage tracing identifies in situ Kit-expressing cardiomyocytes** *Cell Res* **26**:119–130 https://doi.org/10.1038/cr.2015.143

20. Gribben C., Sancho R., Behrens A (2023) **Response to Magenheim et al.: Ductal Ngn3-expressing progenitors contribute to adult beta cell neogenesis in the pancreas** *Cell Stem Cell* **30**:345–347 https://doi.org/10.1016/j.stem.2023.03.002

21. Furuyama K. *et al.* (2011) **Continuous cell supply from a Sox9-expressing progenitor zone in adult liver, exocrine pancreas and intestine** *Nat Genet* **43**:34–41 https://doi.org/10.1038/ng.722

22. Xiao X., Chen Z., Shiota C., Prasadan K., Guo P., El-Gohary Y., Paredes J., Welsh C., Wiersch J., Gittes G (2013) **No evidence for beta cell neogenesis in murine adult pancreas** *J Clin Invest* **123**:2207–2217 https://doi.org/10.1172/JCI66323

23. Tarlow B. D., Finegold M. J., Grompe M (2014) **Clonal tracing of Sox9+ liver progenitors in mouse oval cell injury** *Hepatology* **60**:278–289 https://doi.org/10.1002/hep.27084

24. He L., Nguyen N. B., Ardehali R., Zhou B (2020) **Heart Regeneration by Endogenous Stem Cells and Cardiomyocyte Proliferation: Controversy, Fallacy, and Progress** *Circulation* **142**:275–291 https://doi.org/10.1161/CIRCULATIONAHA.119.045566

25. Liu Q. *et al.* (2019) **Lung regeneration by multipotent stem cells residing at the bronchioalveolar-duct junction** *Nat Genet* **51**:728–738 https://doi.org/10.1038/s41588-019-0346-6

26. He L. *et al.* (2017) **Enhancing the precision of genetic lineage tracing using dual recombinases** *Nat Med* **23**:1488–1498 https://doi.org/10.1038/nm.4437

27. Anastassiadis K., Fu J., Patsch C., Hu S., Weidlich S., Duerschke K., Buchholz F., Edenhofer F., Stewart A. F (2009) **Dre recombinase, like Cre, is a highly efficient site-specific recombinase in E. coli, mammalian cells and mice** *Dis Model Mech* **2**:508–515 https://doi.org/10.1242/dmm.003087

28. Han M. *et al.* (2023) **Dual genetic tracing reveals a unique fibroblast subpopulation modulating cardiac fibrosis** *Nat Genet* **55**:665–678 https://doi.org/10.1038/s41588-023-01337-7

29. Zhang H. *et al.* (2016) **Endocardium Minimally Contributes to Coronary Endothelium in the Embryonic Ventricular Free Walls** *Circ Res* **118**:1880–1893 https://doi.org/10.1161/CIRCRESAHA.116.308749

30. Huelsken J., Vogel R., Erdmann B., Cotsarelis G., Birchmeier W (2001) **beta-Catenin controls hair follicle morphogenesis and stem cell differentiation in the skin** *Cell* **105**:533–545

31. Pontes-Quero S. *et al.* (2017) **Dual ifgMosaic: A Versatile Method for Multispectral and Combinatorial Mosaic Gene-Function Analysis** *Cell* **170**:800–814 https://doi.org/10.1016/j.cell.2017.07.031

32. Kim G. B. *et al.* (2019) **Rapid Generation of Somatic Mouse Mosaics with Locus-Specific, Stably Integrated Transgenic Elements** *Cell* **179**:251–267 https://doi.org/10.1016/j.cell.2019.08.013

33. Zong H., Espinosa J. S., Su H. H., Muzumdar M. D., Luo L (2005) **Mosaic analysis with double markers in mice** *Cell* **121**:479–492 https://doi.org/10.1016/j.cell.2005.02.012

34. Liu C. *et al.* (2011) **Mosaic analysis with double markers reveals tumor cell of origin in glioma** *Cell* **146**:209–221 https://doi.org/10.1016/j.cell.2011.06.014

35. Li Y. *et al.* (2018) **Genetic Lineage Tracing of Non-Myocyte Population by Dual Recombinases** *Circulation* **138**:793–805 https://doi.org/10.1161/CIRCULATIONAHA.118.034250

36. Liu K. *et al.* (2020) **Triple-cell lineage tracing by a dual reporter on a single allele** *J Biol Chem* **295**:690–700 https://doi.org/10.1074/jbc.RA119.011349

37. Zhang H. *et al.* (2016) **Endocardium Contributes to Cardiac Fat** *Circ Res* **118**:254–265 https://doi.org/10.1161/CIRCRESAHA.115.307202

38. Paxinou E., Chen Q., Weisse M., Giasson B. I., Norris E. H., Rueter S. M., Trojanowski J. Q., Lee V. M., Ischiropoulos H (2001) **Induction of alpha-synuclein aggregation by intracellular nitrative insult** *J Neurosci* **21**:8053–8061 https://doi.org/10.1523/JNEUROSCI.21-20-08053.2001

39. Jiang P., Ren L., Zhi L., Hu X., Xiao R. P (2021) **Protocol for cell preparation and gene delivery in HEK293T and C2C12 cells** *STAR Protoc* **2** https://doi.org/10.1016/j.xpro.2021.100497

40. Pu W. *et al.* (2023) **Bipotent transitional liver progenitor cells contribute to liver regeneration** *Nat Genet* **55**:651–664 https://doi.org/10.1038/s41588-023-01335-9

41. Charni-Natan M., Goldstein I (2020) **Protocol for Primary Mouse Hepatocyte Isolation** *STAR Protoc* **1** https://doi.org/10.1016/j.xpro.2020.100086

42. Pu W. *et al.* (2016) **Mfsd2a+ hepatocytes repopulate the liver during injury and regeneration** *Nat Commun* **7** https://doi.org/10.1038/ncomms13369

## Editors

Reviewing Editor
**Michael Potente**
Max Planck Institute for Heart and Lung Research, Bad Nauheim, Germany

Senior Editor
**Didier Stainier**
Max Planck Institute for Heart and Lung Research, Bad Nauheim, Germany

**Reviewer #1 (Public Review):**

Summary:

Shi and colleagues report the use of modified Cre lines in which the coding region of Cre is disrupted by rox-STOP-rox or lox-STOP-lox sequences to prevent the expression of functional protein in the absence of Dre or Cre activity, respectively. The main purpose of these tools is to enable intersectional or tamoxifen-induced Cre activity with minimal or no leaky activity from the second, Cre-expressing allele. It is a nice study but lacks some functional data required to determine how useful these alleles will be in practice, especially in comparison with the figure line that stimulated their creation.

Strengths:

The new tools can reduce Cre leak in vivo.

Weaknesses:

(1) Activity of R26-loxCre line. As the authors point out, the greatest value of this approach is to accomplish a more complete Cre-mediated gene deletion using CreER transgenes that are combined with low-efficiency floxed alleles using their R26-loxCre line that is similar to the iSure Cre reported by Benedito and colleagues. The data in Figure 5 show strong activity at the Confetti locus, but the design of the newly reported R26-loxCre line lacks a WPRE sequence that was included in the iSure-Cre line to drive very robust protein expression. Thus while the line appears to have minimal leak, as the design would predict, the question of how much of a deletion increase is obtained over simple use of the CreER transgene alone is a key question for use by investigators. This is further addressed in Figure 6 where it is compared with Alb-CreER alone to recombine the Ctnnb1 floxed allele. They demonstrate that recombination frequency is clearly improved, but the western blot in Figure 6E does not look like there was a large amount of remaining b-catenin to remove. These data are certainly promising, but the most valuable experiment for such a new tool would be a head-to-head comparison with iSure (or the latest iSure version from the Benedito lab) using the same CreER and target floxed allele. At the very least a comparision of Cre protein expression between the two lines using identical CreER activators is needed.

(2) In vivo analysis of mCre activities. Why did the authors not use the same driver to compare mCre 1, 4, 7, and 10? The study in Figure 2 uses Alb-roxCre for 1 and 7 and Cdh5-roxCre for 4 and 10, with clearly different levels of activity driven by the two alleles in vivo. Thus whether mCre1 is really better than mCre4 or 10 is not clear.

(3) Technical details are lacking. The authors provide little specific information regarding the precise way that the new alleles were generated, i.e. exactly what nucleotide sites were used and what the sequence of the introduced transgenes is. Such valuable information must be gleaned from schematic diagrams that are insufficient to fully explain the approach.

https://doi.org/10.7554/eLife.97717.1.sa2

**Reviewer #2 (Public Review):**

Summary:

This work presents new genetic tools for enhanced Cre-mediated gene deletion and genetic lineage tracing. The authors optimise and generate mouse models that convert temporally controlled CreER or DreER activity to constitutive Cre expression, coupled with the expression of tdT reporter for the visualizing and tracing of gene-deleted cells. This was achieved by inserting a stop cassette into the coding region of Cre, splitting it into N- and C-terminal segments. Removal of the stop cassette by Cre-lox or Dre-rox recombination results in the generation of modified Cre that is shown to exhibit similar activity to native Cre. The authors further demonstrate efficient gene knockout in cells marked by the reporter using these tools, including intersectional genetic targeting of pericentral hepatocytes.

Strengths:

The new models offer several important advantages. They enable tightly controlled and highly effective genetic deletion of even alleles that are difficult to recombine. By coupling Cre expression to reporter expression, these models reliably report Cre-expressing i.e. gene-targeted cells, and circumvent false positives that can complicate analyses in genetic mutants relying on separate reporter alleles. Moreover, the combinatorial use of Dre/Cre permits intersectional genetic targeting, allowing for more precise fate mapping.

Weaknesses:

The scenario where the lines would demonstrate their full potential compared to existing models has not been tested. Mosaic genetics is increasingly recognized as a key methodology for assessing cell-autonomous gene functions. The challenge lies in performing such experiments, as low doses of tamoxifen needed for inducing mosaic gene deletion may not be sufficient to efficiently recombine multiple alleles in individual cells while at the same time accurately reporting gene deletion. Therefore, a demonstration of the efficient deletion of multiple floxed alleles in a mosaic fashion would be a valuable addition.

In addition, a drawback of this line is the constitutive expression of Cre. When combined with the confetti line, the reporter cassette will continue flipping, potentially leading to misleading lineage tracing results. Constitutive expression of Cre is also associated with toxicity, as discussed by the authors in the introduction. These drawbacks should be acknowledged.

https://doi.org/10.7554/eLife.97717.1.sa1

**Reviewer #3 (Public Review):**

Summary:

The authors report a new version of the iSuRe-Cre approach, which was originally developed by Rui Benedito's group in Spain (https://doi.org/10.1038/s41467-019-10239-4). Shi et al claim that their approach shows reduced leakiness compared to the iSuRe-Cre line. Shi et al elaborate strongly about the leakiness of iSuRe-Cre mice, although leakiness is rather minor according to the original publication and the senior author of the study wrote in a review a few years ago that there is no leakiness (https://doi.org/10.1016/j.jbc.2021.100509). Furthermore, a new R26-roxCre-tdT mouse line was established after extensive testing, which enables efficient expression of the Cre recombinase after activation of the Dre recombinase.

Strengths:

The authors carefully evaluated the efficiency and leakiness of the new strains and demonstrated the applicability by marking peri-central hepatocytes in an intersectional genetics approach, amongst others. I can only find very few weaknesses in the paper, which represents the result of an enormous effort. Carefully conducted technical studies have

considerable value. However, I would have preferred to see a study, which uses the wonderful new tools to address a major biological question, rather than a primarily technical report, which describes the ongoing efforts to further improve Cre and Dre recombinase-mediated recombination.

Weaknesses:

Very high levels of Cre expression may cause toxic effects as previously reported for the hearts of Myh6-Cre mice. Thus, it seems sensible to test for unspecific toxic effects, which may be done by bulk RNA-seq analysis, cell viability, and cell proliferation assays. It should also be analyzed whether the combination of R26-roxCre-tdT with the Tnni3-Dre allele causes cardiac dysfunction, although such dysfunctions should be apparent from potential changes in gene expression.

The R26-GFP or R26-tdT reporters, Alb-roxCre1-tdT, Cdh5-roxCre4-tdT, Alb-roxCre7-GFP, and Cdh5-roxCre10-GFP demonstrate no leakiness without Dre-rox recombination (Figure S1-S2). Is there any leakiness when the inducible DreER allele is introduced but no tamoxifen treatment is applied? This should be documented. The same also applies to loxCre mice.

The enhanced efficiency of loxCre and roxCre systems holds promise for reducing the necessary tamoxifen dosage, potentially reducing toxicity and side effects. In Figure 6, the author demonstrates an enhanced recombination efficiency of loxCre mice, which makes it possible to achieve efficient deletion of Ctnnb1 with a single dose of tamoxifen, whereas a conventional driver (Alb-CreER) requires five dosages. It would be very helpful to include a dose-response curve for determining the minimum dosage required in Alb-CreER; R26-loxCre-tdT; Ctnnb1flox/flox mice for efficient recombination.

In the liver panel of Figure 4F, tdT signals do not seem to colocalize with the VE-cad signals, which is odd. Is there any compelling explanation?

The authors claim that "virtually all tdT+ endothelial cells simultaneously expressed YFP/mCFP" (right panel of Figure 5D). Well, it seems that the abundance of tdT is much lower compared to YFP/mCFP. If the recombination of R26-Confetti was mainly triggered by R26-loxCre-tdT, the expression of tdT and YFP/mCFP should be comparable. This should be clarified.

In several cases, the authors seem to have mixed up "R26-roxCre-tdT" with "R26-loxCre-tdT". There are errors in #251 and #256. Furthermore, in the passage from line #278 to #301. In the lines #297 and #300 it should probably read "Alb-CreER; R26-loxCre-tdT;Ctnnb1flox/flox"" rather than "Alb-CreER;R26-tdT2;Ctnnb1flox/flox".

https://doi.org/10.7554/eLife.97717.1.sa0

Author response:

**Response letter**

> ***Public Reviews:***
>
> ***Reviewer #1 (Public Review):***
>
> *(1) It is a nice study but lacks some functional data required to determine how useful these alleles will be in practice, especially in comparison with the figure line that stimulated their creation.*

We are grateful for this comment. For the usefulness of these alleles, figure 3 shows that specific and efficient genetic manipulation of one cell subpopulation can be achieved by mating across the *DreER* mouse strain to the *rox-Cre* mouse strain. In addition, figure 6 shows that *R26-loxCre-tdT* can effectively ensure Cre-loxP recombination on some gene alleles and for genetic manipulation. The expression of the tdT protein is aligned with the expression of the Cre protein (Alb roxCre-tdT and R26-loxCre-tdT, figure 2 and figure 5), which ensures the accuracy of the tracing experiments. We believe more functional data can be shown in future articles that use mice lines mentioned in this manuscript.

> *(2) The data in Figure 5 show strong activity at the Confetti locus, but the design of the newly reported R26-loxCre line lacks a WPRE sequence that was included in the iSure-Cre line to drive very robust protein expression.*

Thank you for coming up with this point in the manuscript. In the *R26-loxCre-tdT* mice knock-in strategy, the WPRE sequence is added behind the *loxCre-P2A-tdT* sequence.

> *(3) the most valuable experiment for such a new tool would be a head-to-head comparison with iSure (or the latest iSure version from the Benedito lab) using the same CreER and target foxed allele. At the very least a comparison of Cre protein expression between the two lines using identical CreER activators is needed.*

According to the reviewer's suggestion, we will compare *iSuRe-Cre* with *R26-loxCre-tdT* by using *Alb-CreER* and target *R26-Confetti* in the revised manuscript.

> *(4) Why did the authors not use the same driver to compare mCre 1, 4, 7, and 10? The study in Figure 2 uses Alb-roxCre for 1 and 7 and Cdh5-roxCre for 4 and 10, with clearly different levels of activity driven by the two alleles in vivo. Thus whether mCre1 is really better than mCre4 or 10 is not clear.*

Thank you for raising this concern. After screening out four robust versions of mCre, we generated these four roxCre knock-in mice. It is unpredictable for us which is the most robust mCre *in vivo*. It might be one or two mCre versions that work efficiently. For example, if *Alb-mCre1* was competitive with *Cdh5-mCre10*, we can use them for targeting genes in different cell types, broadening the potential utility of these mice.

> *(5) Technical details are lacking. The authors provide little specific information regarding the precise way that the new alleles were generated, i.e. exactly what nucleotide sites were used and what the sequence of the introduced transgenes is. Such valuable information must be gleaned from schematic diagrams that are insufficient to fully explain the approach.*

Thank you for your careful suggestions.

We will provide schematic figures as well as nucleotide sequences for mice generation in the revised manuscript.

> ***Reviewer #2 (Public Review):***
>
> *(1) The scenario where the lines would demonstrate their full potential compared to existing models has not been tested.*

We are grateful for this suggestion. We will compare *iSuRe-Cre* with *R26-loxCre-tdT* by using *Alb-CreER* and target *R26-Confetti* in the revised manuscript.

> *(2) The challenge lies in performing such experiments, as low doses of tamoxifen needed for inducing mosaic gene deletion may not be sufficient to efficiently recombine multiple alleles in individual cells while at the same time accurately reporting gene deletion. Therefore, a demonstration of the efficient deletion of multiple floxed alleles in a mosaic fashion would be a valuable addition.*

Thank you for your constructive comments. Mosaic analysis using sparse labeling and efficient gene deletion would be our future direction using roxCre and loxCre strategies. We will include some discussion of using such strategy in the revised manuscript.

> *(3) When combined with the confetti line, the reporter cassette will continue flipping, potentially leading to misleading lineage tracing results.*

Thank you for your professional comments. Indeed, the confetti used in this study can continue flipping, which would lead to potentially misleading lineage tracing results. Our use of R26-Confetti is to demonstrate the robustness of mCre for recombination. Some multiple-color mice lines that don't flip have been published, for example, R26-Confetti2(10.1038/s41588-019-0346-6) and Rainbow (10.1161/CIRCULATIONAHA.120.045750). These reporters could be used for tracing Cre-expressing cells, without concerns of flipping of reporter cassettes.

> *(4) Constitutive expression of Cre is also associated with toxicity, as discussed by the authors in the introduction.*

Thank you for your professional comments. The toxicity of constitutive expression of Cre and the toxicity associated with tamoxifen treatment in CreER mice line (10.1038/s44161-022-00125-6) are known to the field. This study can't solve the toxicity of the constitutive expression of Cre in this work. Many mouse lines with constitutive Cre driven by different promoters are present across various fields, representing similar toxicity. To solve this issue, it would be possible to construct a new strategy that enables the removal of Cre after its expression.

> ***Reviewer #3 (Public Review):***
>
> *(1) Although leakiness is rather minor according to the original publication and the senior author of the study wrote in a review a few years ago that there is no leakiness(https://doi.org/10.1016/j.jbc.2021.100509).*

Thank you so much for your careful check. In this review (https://doi.org/10.1016/j.jbc.2021.100509), the writer's comments on *iSuRe-Cre* are on the reader's side, and all summary words are based on the original published paper (10.1038/s41467-019-10239-4). Currently, we have tested *iSuRe-Cre* in our hands. We did detect some leakiness in the heart and muscle, but hardly in other tissues as shown in the following figure.

**Author response image 1.**

Leakiness in *Alb CreER*;*iSuRe-Cre* mouse line. Pictures are representative results for 5 mice. Scale bars, white 100 μm.

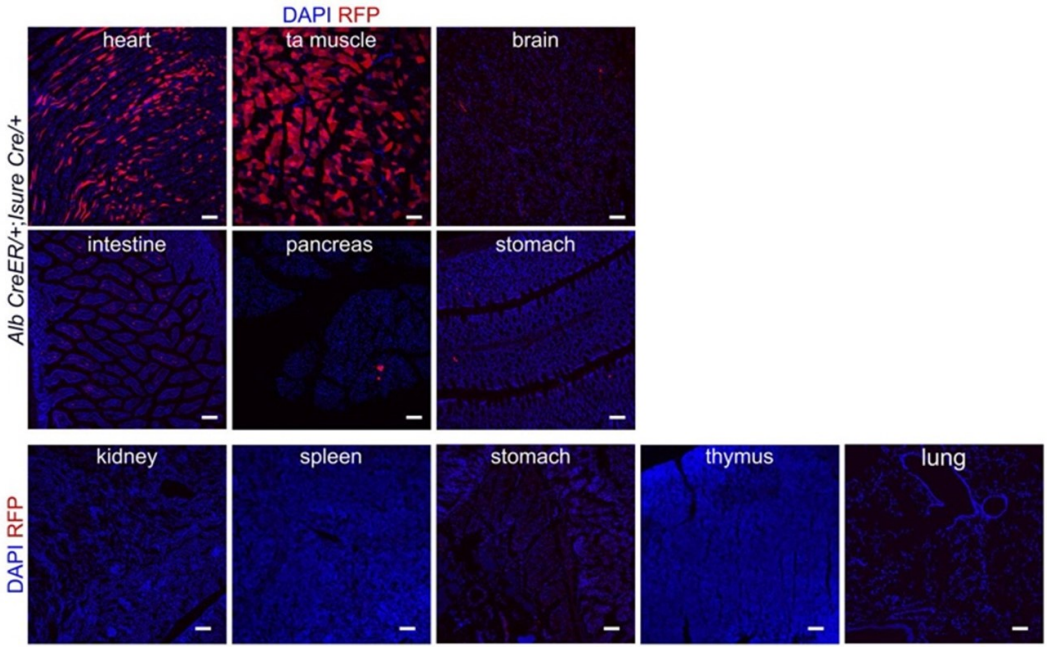


> *(2) I would have preferred to see a study, which uses the wonderful new tools to address a major biological question, rather than a primarily technical report, which describes the ongoing efforts to further improve Cre and Dre recombinase-mediated recombination.*

We gratefully appreciate your valuable comment. The roxCre and loxCre mice mentioned in this study provide more effective methods for inducible genetic manipulation in studying gene function. We hope that the application of our new genetic tools could help address some major biological questions in different biomedical fields in the future.

> *(3) Very high levels of Cre expression may cause toxic effects as previously reported for the hearts of Myh6-Cre mice. Thus, it seems sensible to test for unspecific toxic effects, which may be done by bulk RNA-seq analysis, cell viability, and cell proliferation assays. It should also be analyzed whether the combination of R26-roxCre-tdT with the Tnni3-Dre allele causes cardiac dysfunction, although such dysfunctions should be apparent from potential changes in gene expression.*

We are sorry that we mistakenly spelled R26-loxCre-tdT into R26-roxCre-tdT in our manuscript. We have not generated R26-roxCre-tdT mouse line. We also thank the reviewer for concerns about the toxicity of high Cre expression. The toxicity of constitutive expression of Cre and the toxicity of tamoxifen treatment of CreER mice line (10.1038/s44161-022-00125-6) are known to the field. This study can't solve the toxicity of the constitutive expression of Cre in this work. Many mouse lines with constitutive Cre driven by different promoters are present across various fields, representing similar toxicity. To solve this issue, it would be possible to construct a new strategy that enables the removal of Cre after its expression.

> *(4) Is there any leakiness when the inducible DreER allele is introduced but no tamoxifen treatment is applied? This should be documented. The same also applies to loxCre mice.*

In this study, we come up with new mice tool lines, including *Alb roxCre1-tdT*, *Cdh5 roxCre4-tdT*, *Alb roxCre7-GFP*, *Cdh5 roxCre10-GFP* and *R26-loxCre-tdT*. As the data shown in supplementary figure 1, supplementary figure 2, and figure 4D, *Alb roxCre1-tdT*, *Cdh5 roxCre4-tdT*, *Alb roxCre7-GFP*, *Cdh5 roxCre10-GFP* and *R26-loxCre-tdT* are not leaky.

Therefore, if there is any leakiness driven by the inducible DreER or CreER allele, the leakiness is derived from the DreER or CreER. We will supplement relevant experimental data in the revision.

> *(5) It would be very helpful to include a dose-response curve for determining the minimum dosage required in Alb-CreER; R26-loxCre-tdT; Ctnnb1flox/flox mice for efficient recombination.*

Thank you for your suggestion. We understand the reviewer's concern. We can do a dose-response curve in the revision work.

> *(6) In the liver panel of Figure 4F, tdT signals do not seem to colocalize with the VE-cad signals, which is odd. Is there any compelling explanation?*

As the file-loading website has a file size limitation, the compressed image results in some signal unclear. The following are the zoom-out figures. The staining in Figure 4F will be optimized and high-resolution images will be provided in the revision.

**Author response image 2.**

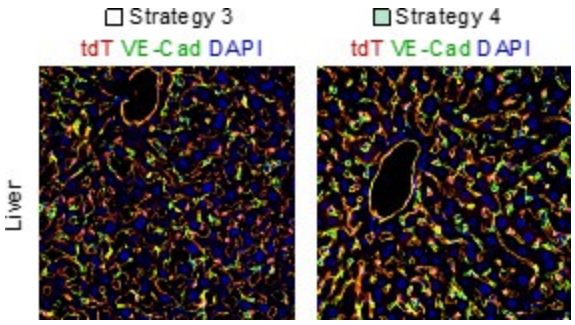


> *(7) The authors claim that "virtually all tdT+ endothelial cells simultaneously expressed YFP/mCFP" (right panel of Figure 5D). Well, it seems that the abundance of tdT is much lower compared to YFP/mCFP. If the recombination of R26-Confetti was mainly triggered by R26-loxCre-tdT, the expression of tdT and YFP/mCFP should be comparable. This should be clarified.*

Thank you so much for your careful check. We checked these signals carefully and didn't find the "much lower" tdT signal. As the file-loading website has a file size limitation, the compressed image results in some signal unclear. We attached clear high resolution images here. The following figure shows how we split the tdT signal and compared it with YFP/mCFP.

**Author response image 3.**

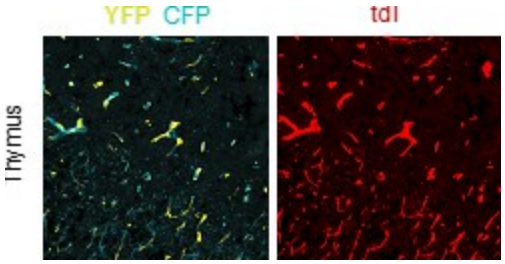

> *(8) In several cases, the authors seem to have mixed up "R26-roxCre-tdT" with "R26-loxCre-tdT". There are errors in #251 and #256.Furthermore, in the passage from line #278 to #301. In the lines #297 and #300 it should probably read "Alb-CreER; R26-loxCretdT;Ctnnb1flox/flox"" rather than "Alb-CreER;R26-tdT2;Ctnnb1flox/flox".*

We are grateful for these careful observations. We have corrected these typos accordingly.

https://doi.org/10.7554/eLife.97717.1.sa4